LBL-23282
Preprint

Lawrence Berkeley Laboratory
UNIVERSITY OF CALIFORNIA

Materials & Chemical Sciences Division

RECEIVED
LIBRARY
JUL 9 1987
DOCUMENTS SECTION

Center for Advanced Materials

Submitted to Journal of Applied Physics

SOLID PHASE REACTIONS BETWEEN (100) GaAs AND THIN FILM REFRACTORY METALS (Ti, Zr, V, Nb, Cr, Mo and W)

K.M. Yu, J.M. Jaklevic, and E.E. Haller

April 1987

TWO-WEEK LOAN COPY
This is a Library Circulating Copy
which may be borrowed for two weeks

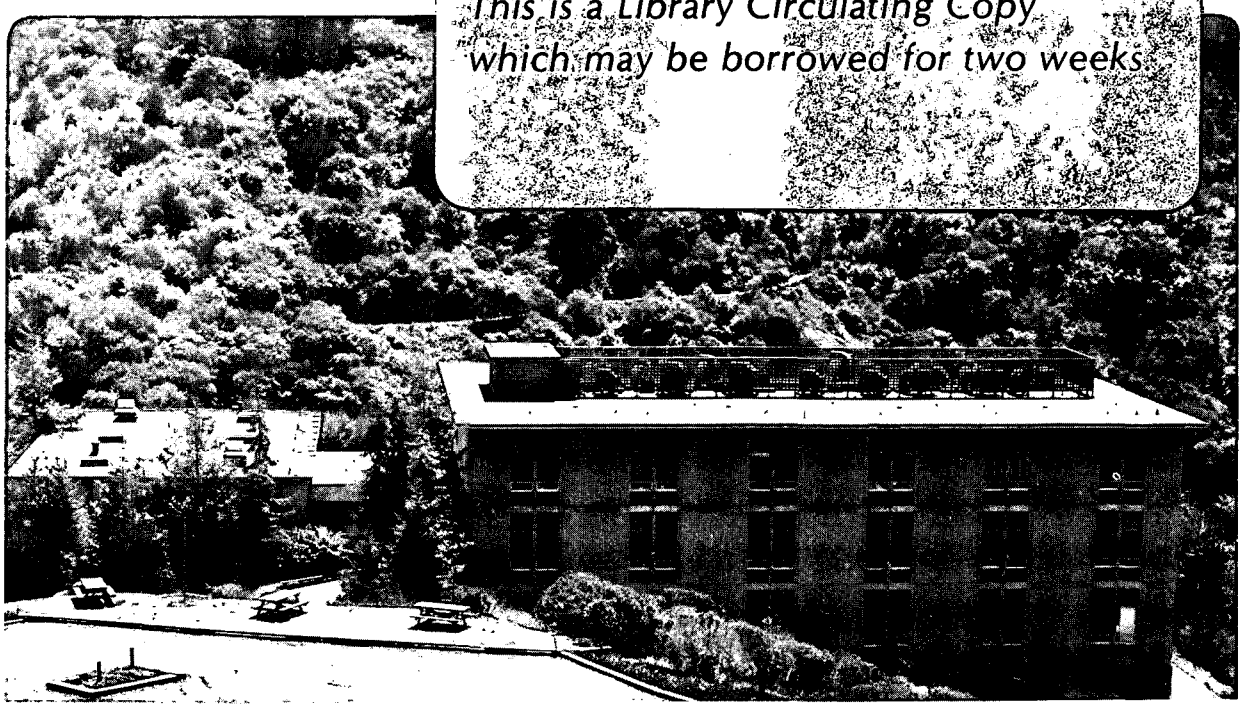

LBL-23282 c.2

Prepared for the U.S. Department of Energy under Contract DE-AC03-76SF00098

DISCLAIMER

This document was prepared as an account of work sponsored by the United States Government. While this document is believed to contain correct information, neither the United States Government nor any agency thereof, nor the Regents of the University of California, nor any of their employees, makes any warranty, express or implied, or assumes any legal responsibility for the accuracy, completeness, or usefulness of any information, apparatus, product, or process disclosed, or represents that its use would not infringe privately owned rights. Reference herein to any specific commercial product, process, or service by its trade name, trademark, manufacturer, or otherwise, does not necessarily constitute or imply its endorsement, recommendation, or favoring by the United States Government or any agency thereof, or the Regents of the University of California. The views and opinions of authors expressed herein do not necessarily state or reflect those of the United States Government or any agency thereof or the Regents of the University of California.

SOLID PHASE REACTIONS BETWEEN (100) GaAs AND THIN FILM REFRACTORY METALS (Ti, Zr, V, Nb, Cr, Mo and W)

K. M. Yu, J. M. Jaklevic and E. E. Haller

Center for Advanced Materials and Engineering Division,

Lawrence Berkeley Laboratory, University of California, Berkeley,

Berkeley, California 94720

ABSTRACT

Recently, there has been an increased interest in the applications of refractory metals as gate materials for the self aligned gate process in the fabrications of GaAs field effect transistors. In this study, we systematically investigated the thermally induced interface interactions between (100) GaAs substrates and thin films of refractory metals (Ti, Zr, V, Nb, Cr, Mo and W). Depth profilings of the M/GaAs interfaces were obtained using conventional and heavy ion Rutherford backscattering spectrometry. Phase identifications were achieved by x-ray diffraction.

Results on the phase formation sequence, reaction kinetics, the distribution, composition and structure of the reacted phases and the interface reactivity of these contacts will be presented. Correlations between metal properties (electronegativity and metal-metal bond strength) and kinetics of the reactions (activation energy and reactivity of the interfaces) will also be discussed.

I. INTRODUCTION

The interest in high-speed and high density metal/GaAs MESFET (metal-semiconductor field effect transistor) integrated circuits has stimulated the development of new device processing concepts which are simple and compatible with future GaAs IC scaling. The self-aligned gate (SAG) technique is one of such new concepts. The success of the SAG technique in the fabrication of GaAs MESFETs has been reported[1]. In the SAG process, the gate is used as an implantation mask for the formation of the source and drain regions. Implantation is followed by a high temperature annealing step (>850°C). This requires thermally stable (up to at least 900°C) and electrically reproducible GaAs Schottky contacts.

In the last five years, many investigators have explored the thermal stability of refractory metals[2] as well as the alloys[3], silicides[4-9] and nitrides[10-13] of refractory metals as gate materials for SAG GaAs MESFET. Despite all these studies focussing on the exploration of suitable gate materials for SAG GaAs MESFETs, very little is known about the interactions at the refractory metal/GaAs interfaces. In order to select better gate materials for GaAs SAG-MESFET in the future, the interfacial metallurgy of refractory metal/GaAs contact systems must be well understood.

Studies on the solid phase reactions of refractory metal/GaAs contacts, such as Ti/GaAs[14], Cr/GaAs[15,16], Mo/GaAs[15-18] and W/GaAs[15,16,19] have been reported in the literature. However, no attempt on the study of the systematics of these reactions has been made. Hence, these results only provide a preliminary understandings of the refractory metal/GaAs interfaces. In the present study, we systematically investigated the solid

phase reactions between (100) GaAs and thin films of refractory metals including titanium, zirconium, vanadium, niobium, chromium, molybdenum and tungsten. Measurements were performed using conventional and heavy ion Rutherford backscattering spectrometry (RBS and HIRBS) and x-ray powder diffractometry (XRD). Issues such as reaction kinetics, interface reactivity as well as the distribution, composition and stabiltiy of the reacted phases will be discussed.

II. EXPERIMENTAL

Undoped (100) GaAs wafers with $\rho > 10^7$ Ω-cm (Wacker Chemitronic) were degreased by boiling in trichloroethane, acetone and methanol for 5 min each. The wafers were then etched in a 50% HCl solution for 1 min in order to reduce the thickness of the native oxide on the GaAs surface. Thin films (100-1500 Å) of V, Cr and Mo were deposited on the wafer by electron gun evaporation in a chamber with base pressure below 10^{-6} Torr. Films of Ti, Zr, Nb and W were sputter deposited onto the GaAs substrates at an argon pressure of ~15 mTorr. The samples were capped on both sides with ~1500 Å of SiO_2 films deposited by plasma enhanced chemical vapor deposition at a substrate temperature of ~150°C. Annealing was carried out in the temperature range from 300 to 900°C for various lengths of time in a flowing N_2 ambient. The oxide caps were then removed by dipping the samples in a solution of buffered HF solution for ~3 min.

Both conventional RBS and HIRBS measurements have been carried out on thin film refractory metal/GaAs systems. A 20 MeV $^{16}O^{++}$ beam generated by the 88" cyclotron at the Lawrence Berkeley Laboratory was used for HIRBS

measurements. Details of the HIRBS technique have been described in References 20 and 21. Conventional RBS measurements were performed with 2.0 MeV α particles generated by the 2 MeV Van de Graaff at LBL. For very thin layers with a thickness < 150 Å, samples were mounted on a goniometer and tilted to an incident angle > 50° with respect ot the specimen normal in order to improve depth resolution.

X-ray diffraction (XRD) experiments were performed in the Bragg-Brentano focusing geometry where the diffraction peaks were recorded by a detector scanning through Bragg angle 2θ, ranging from 10 to 100°. Phase identification was achieved by matching the detected diffraction peaks with x-ray powder diffraction data files. XRD in this geometry is sensitive to films with thicknesses ≥300 Å.

III. RESULTS AND DISCUSSIONS

Table I shows a summary of the experimental results. Details and discussions on these results will be presented in the following sections. Since the results of the W/GaAs study have been published[19], they will be discussed only briefly here for comparative purposes.

1. Ti/GaAs

We observe a reaction between a Ti thin film and the GaAs substrate at annealing temperatures above 400°C. Figure 1 shows the results of the HIRBS measurements on 1000 Å Ti/GaAs samples as deposited and annealed at 450 and 500°C for 20 min. After annealing at 500°C for 20 min the Ti film is completely consumed by reacting with the GaAs substrate. Deconvolution

of the HIRBS spectrum from the sample annealed at 500°C (Figure 1(b)) indicates a two layer phase sequence with the top layer composed primarily of Ti and Ga and the interface layer consisting of Ti and As. From the energy loss characteristics of the ^{16}O projectiles in Ti and GaAs, the atomic ratio of the reacted [Ti]:[GaAs] is estimated to be 2:1. Ratios of the backscattering yields from the individual element in the HIRBS spectrum gives [Ti]:[Ga]≈1:1 for the top layer and [Ti]:[As]≈1:1 for the layer at the interface. The presence of a large amount of As signals in the top layer in the spectrum indicates that the interface between the TiGa and TiAs phases is non-abrupt. XRD spectra of samples of Ti/GaAs annealed at 450 and 500°C for 20 min show that the products of thermally activated Ti/GaAs reactions in this temperature range are hexagonal TiAs (a_o=3.64 Å and c_o=12.06 Å) with 8 atoms per unit cell and tetragonal TiGa (a_o=c_o=3.97 Å). A summary of the XRD data together with the X-ray powder diffraction data from TiGa and TiAs standards are given in Table II.

HIRBS spectra of samples annealed at 500°C for longer times show that the Ga and As signals in the two layers start to intermix but without further consumption of the GaAs substrate. Moreover, no new phase is detectable in these samples by XRD. This can be interpreted as the effect of more interpenetration between the two phases which make their interface very "rough". We believe that the interpenetration of phases at the interface is due to grain growth of the phases during extended annealing time. Further annealing at temperatures higher than 500°C (up to 800°C) does not result in new features in the HIRBS and XRD spectra. Therefore, TiGa and TiAs are the only and final products for the solid phase reactions between thin film Ti and GaAs with the layer sequence of TiGa/TiAs/GaAs when a short annealing time is used (≤20 min).

Using sputtering Auger electron spectroscopy (AES) and XRD, Wada et al[14] reported a layer sequence of Ti-Ga/Ti-As/GaAs as a result of Ti/GaAs reactions at elevated temperatures. This is consistent with the HIRBS results in the present study. They observed the presence of TiAs and Ti_2Ga_3 phases in samples of Ti/GaAs annealed at 480°C. At higher annealing temperatures, they also found Ti_5Ga_4 and Ti_5As_3 phases in addition to the other two phases. Since no capping has been applied to the Ti/GaAs samples during annealing in the study by Wada et al, it is likely that excess vaporization of arsenic at elevated temperatures resulted in the formation of As deficient phases. However, with a limited amount of Ti (thin film) and a quasi-unlimited amount of GaAs, it is doubtful that the reaction will be driven from the more Ga (As) rich Ti_2Ga_3 (TiAs) phase(s) to the more Ti rich Ti_5Ga_4 (Ti_5As_3) phase(s).

We also studied the reaction kinetics of the Ti/GaAs system using HIRBS. The reaction rate of the Ti/GaAs interface is found to be dependent on the square root of annealing time t, i. e. dominated by a diffusion process. The activation energy for the reactions is estimated from reaction rate curves and equals 1.53±0.15 eV. These kinetics are in good agreement with those measured by Wada et al who reported a slightly higher ΔE of 1.70 eV. However, it should be pointed out that the AES technique employed by Wada et al for depth profiling is not quantitative and therefore depth information obtained by this method without appropriate standard cannot be considered accurate.

2. Zr/GaAs

Interdiffusion at the Zr/GaAs interface is observed by HIRBS at temperatures around 450°C. Figure 2 shows the results of the HIRBS measurements on 1100 Å Zr/GaAs samples as deposited and annealed at different temperatures. Deconvolution of these spectra are difficult due to the good mass resolution of HIRBS which partially resolves the different isotopes of Zr. In other words, the effects of the multiple isotopes of Zr on the HIRBS spectra are similar to those of an alloy film composed of many elements with similar masses. The spectra in Figure 2 show that the reactions at the Zr/GaAs interface proceed very slowly. The reactions are completed only after annealing at 700°C for 60 min. The atomic ratio of Zr and GaAs in this final stage of reaction is measured by HIRBS and is ≈2:1. An intermediate stage in the Zr/GaAs reactions with [Zr]:[GaAs]≈3:1 is also observed at annealing temperatures around 650-700°C. The relatively long annealing time required for reactions in this system promotes significant grain growth in the reacted layer. This is manifested by the absence of phase stratification as noticed in the HIRBS spectra.

Results of XRD measurements on the same set of samples are tabulated in Table III. X-ray powder diffraction data on a Zr_5Ga_3 standard are also shown in the table. The Zr_5Ga_3 standard data match well with some of the diffraction peaks in the XRD spectrum from the sample annealed at 700°C for 60 min. Therefore, we conclude that one of the reacted final phase is Zr_5Ga_3. Because of the lack of x-ray powder diffraction and equilibrium thermodynamic data for Zr-As phases, identification of Zr-As phase(s) by direct matching of the XRD results is not possible.

Figure 3 shows plots of the square of GaAs consumed (in cm) during reactions as measured by HIRBS versus annealing time for different annealing temperatures. The linear relationships shown in these plots indicates that all reactions are diffusion controlled. The activation energy of the reactions is estimated from the slope of the Arrhenius plot shown in Figure 4 and is 1.25±0.15 eV. The value of this energy is low compared to those obtained for other metal/GaAs systems.

Since minimization of the free energy G is the driving force for a given reaction, the free energy change ΔG is of primary interest. From basic thermodynamics, ΔG can be expressed as:

$$\Delta G = \Delta E - T\Delta S$$

where T is the temperature and ΔS is the activation entropy of the reaction. Therefore, from the kinetic theory, the reaction rate can be written as:

$$\frac{dx}{dt} = K\exp\left(\frac{-\Delta G}{kT}\right) = K\exp\left(\frac{\Delta S}{k}\right)\exp\left(\frac{-\Delta E}{kT}\right), \qquad (1)$$

where K is a constant dependent on the frequency with which particles attempt to transform and the probability that during the time a particle or particles have the required energy to satisfy the geometrical or other conditions necessary for the change. The slow reactions rate observed in this system despite its small activation energy thus lets us infer that the activation entropy ΔS for the Zr/GaAs reactions must be strongly negative so that the $\exp(\Delta S/k)$ term dominates in equation (1).

3. V/GaAs

Chemical reactions are detected at the V/GaAs interface by HIRBS during annealing at ~450°C. HIRBS spectra of 1500 Å V/GaAs samples as deposited and annealed at 600°C for 20 min and 700°C for 30 min are shown in Figure 5. The entire vanadium film has reacted with the GaAs substrate in the sample annealed at 600°C for 20 min. This is also confirmed by the XRD result on the same sample which shows no diffraction peak corresponding to unreacted V. The V signals in the HIRBS spectra from the two annealed samples indicate that two layer structures are formed in both cases with the top layer richer in vanadium than the interface layer. The presence of Ga signals in both samples at the surface can also be seen. Energy loss analysis shows reacted [V]:[GaAs] ratios ≈5:1 for the the sample annealed at 600°C and ≈2.2:1 for the one annealed at 700°C. Deconvolution of the HIRBS spectra of these two annealed samples are illustrated in Figure 6. Height ratio analysis of the backscattering yield from the individual element results in [V]:[Ga]≈3:1, [V]:[As]≈2:1 and [V]:[Ga]≈1.2:1, [V]:[As]≈ 1.1:1 for the samples annealed at 600°C and 700°C, respectively.

XRD patterns for the sample annealed at 700°C for 30 min match reasonably well with those for hexagonal V_6Ga_5 (a_o=8.496 Å and c_o=5.176 Å) and monoclinic V_4As_3 phase. For the sample annealed at 600°C for 20 min, only the cubic V_3Ga (a_o=4.8153 Å) phase can be identified by XRD. The other diffraction peaks in this XRD spectrum do not match with any of the available standard V-Ga or V-As patterns. From the HIRBS analysis, the other phase present in this sample is most probably V_2As. However, the structure of this V_2As phase is not known.

The HIRBS and XRD results show that the solid-state interactions at the V/GaAs interface proceed in two stages consistent with the following equations:

stage 1: $5\ V + GaAs \rightarrow V_3Ga + V_2As$, and

stage 2: $38V + 15GaAs \rightarrow 3V_6Ga_5 + 5V_4As_3$.

The fact that the ratio of the reacted [V]/[GaAs] for stage 2 reaction as measured by HIRBS is 2.2 instead of 2.5 is believed to be the effect of excessive energy straggling of the oxygen projectiles after passing through a thick layer. Table IV summarizes the HIRBS data for the 2-stage reactions of V/GaAs system. Layer sequence of V-Ga/V-As/GaAs is observed for all reacted layers in this system.

Measurements of the thickness of reacted GaAs in the annealed V/GaAs samples by HIRBS indicate that the reaction rate of this contact system is diffusion limited. The square root of time dependence of GaAs consumption during reaction is plotted in Figure 7. Figure 8 shows an Arrhenius plot of the diffusivities and annealing temperature. The activation energy of the reactions estimated from these data is 2.1±0.1 eV. This high activation energy is consistent with the high annealing temperature (≥450°C) required to induce reactions at the interface.

4. <u>Nb/GaAs</u>

In contrast to the V/GaAs contact system, we observe only one kind of reaction in the Nb/GaAs system. Interactions between niobium metal film and GaAs are detected during annealing at 550°C by HIRBS. Figure 9 shows the HIRBS spectra of 550 Å Nb/GaAs samples as deposited and annealed at 600 and 700°C for 20 min. Complete reaction of the 550 Å of Nb film is

observed in the sample annealed at 700°C for 20 min. The corresponding HIRBS spectrum shows that the surface is depleted of As and is relatively less rich in Nb concentration. The low energy tail of the Nb signal indicates that the interface between the reacted phases and the GaAs substrate is not uniform. Furthermore, the smoothness of the high energy signal of As is an indication of interpenetration of the top Nb-Ga and interface Nb-As phases.

The compositions of the reacted phases cannot be estimated from the HIRBS spectrum. The ratio of the total reacted Nb to GaAs is deduced from the spectrum and lies close to 1.55:1. XRD measurements on the sample annealed at 500°C shows a new set of diffraction peaks in addition to the niobium diffraction peaks. This same set of peaks is also detected in the XRD spectra of the samples annealed at 600°C and 700°C and is observed to grow at the expense of the niobium peaks. This indicates that there is only one set of stable phases in the Nb/GaAs reactions which gives rise to these diffraction peaks in the XRD spectra. However, no good match of this XRD pattern with any of the existing standard x-ray powder diffraction patterns of Nb-Ga and Nb-As phases can be found. From the XRD and HIRBS data, a schematic of the final structure of the Nb/GaAs contact after reactions is illustrated in Figure 10.

The amount of GaAs consumed during Nb/GaAs interface reactions is measured by HIRBS and is found to be dependent on the square root of the annealing time. This indicates that the reactions are controlled by a diffusion process. Because of the high annealing temperature (~550°C) needed in order to induced a solid phase reaction at the Nb/GaAs interface, the activation energy is expected to be high. HIRBS results yield an

activation energy of ≈2.60 eV consistent with the observed annealing behavior of this system.

5. Cr/GaAs

Interdiffusions and interactions at the Cr/GaAs interface are detectable by HIRBS during annealing at temperatures ≥450 °C. A set of HIRBS spectra of 1200 Å Cr/GaAs samples annealed at different conditions are shown in Figure 11. HIRBS spectra of the two annealed samples in the figure represent two stages of complete reactions of this system. Deconvolutions of the spectra from the two annealed samples are given in Figure 12. Layered structures are evident in the HIRBS spectra from both of the annealed samples.

The entire Cr film has reacted with the GaAs substrate in the sample annealed at 550 °C for 10 min. In the HIRBS spectrum of this sample, the ratio of the reacted Cr to GaAs is estimated to be ≈3.9. Deconvolution of this spectrum yields [Cr]:[Ga] ≈3:1 for the top layer and [Cr]:[As] ≈1:1 for the layer at the GaAs interface. These results are consistent with the reaction:

$$4\ Cr + GaAs \rightarrow Cr_3Ga + CrAs,$$

and layer sequence of Cr_3Ga/CrAs/GaAs. These are the first stage reactions in the Cr/GaAs system. The second stage reactions are completed after annealing at 600 °C for 20 min. Deconvolution of the HIRBS spectrum of this sample shown in Figure 12(b) reveals that the composition of the interface layer is similar to that of the stage 1 reactions. However, the [Cr]/[Ga] ratio in the top layer is changed from 3 to 1. Energy loss analysis gives a ratio of the reacted Cr to GaAs of ≈2.2 in this sample. These results are in good agreement with the reaction:

$$2\ Cr + GaAs \rightarrow CrGa + CrAs.$$

The layer sequence detected for this reaction is therefore CrGa/CrAs/GaAs. In both stages of reactions, a significant amount of As (10-20%), probably in the form of CrAs, is found in the top Cr-Ga layer.

Three phases are identified by XRD in Cr/GaAs samples annealed at temperatures between 400°C and 700°C. Cubic Cr_3Ga of the β-W type (a_o=4.645 Å) and orthorhombic CrAs (a_o=3.486 Å, b_o=6.222 Å and c_o=5.741 Å) are the phases formed during stage 1 reactions in the temperature range of 450 to 550°C. At temperatures higher than 550°C, the Cr_3Ga phase becomes unstable and transforms into the more stable rhombohedral CrGa phase (a_o=9.01 Å and α=89°11'). XRD measurements on samples annealed at temperatures higher than 600°C do not show diffraction peaks different from those of the CrGa and CrAs phases. Therefore, the CrGa and CrAs phases are the stable final phases for the thin film Cr/GaAs contact system.

6. Mo/GaAs

HIRBS analysis on Mo/GaAs couples shows that the interface reaction is initiated at temperatures above 650°C. Figure 13 displays a series of HIRBS spectra of 1500 Å Mo/GaAs samples as deposited and annealed at 700°C for 40 min and 140 min. We oberve a well established layer structure in the spectrum of a sample annealed at 700°C for 140 min in which complete reactions of the molybdenum film are observed. Figure 14 gives the deconvolution of this HIRBS spectrum which shows a layer sequence of Mo-Ga/Mo-As/GaAs formed after the reactions. The abruptness of the edges in the HIRBS spectrum suggests that the interface between the two Mo phases and that between GaAs and Mo-As are rather sharp and uniform. This

indicates that the reacted Mo-Ga and Mo-As phases have fine grain structure. Sands et al[22] have explored the relationship between the metal-metal bond srength and the final grain size of the reacted phases for near noble metal/GaAs contacts. They concluded that for metals with strong M-M bonds, and therefore high heat of vaporization, the reacted phases have fine grain structure. This is consistent with the fact that the M-M bond for molybdenum is strong and thus produces fine grains in the reacted layer. In fact, Ling et al[17] measured an average grain size of ~100 Å using TEM for Mo/GaAs samples annealed at 700°C. The XRD spectrum of this sample confirms that the entire Mo film is reacted with the substrate. HIRBS spectra of samples annealed at temperatures ranging from 750 to 850°C are identical to that of the sample annealed at 700°C for 140 min. This indicates that the phases formed at 700°C are thermally very stable.

From the Mo backscattered signal in Figure 14, it is obvious that the top Mo-Ga phase is richer in Mo than the interface Mo-As phase. Ratios of the backscattered yields give [Mo]:[Ga]≈2.5:1 for the top layer and [Mo]:[As]≈1.2:1. XRD results on samples annealed at temperatures ranging from 700 to 850°C show the presence of two phases: the cubic Mo_3Ga (a_o=4.943 Å) and the tetragonal Mo_5As_4 (a_o=9.6 Å and c_o=3.278 Å). The apparent discrepancy in the composition of the Mo-Ga phase as measured by HIRBS and XRD probably stems from the many Mo isotopes which are only partially resolved by HIRBS. This isotopic spread reduces the height of the Mo signals by 15-20%. From the HIRBS and XRD results the structure of Mo_3Ga/Mo_5As_4/GaAs can be deduced for the Mo/GaAs reactions in the temperature range from 700 to 850°C.

Annealing the Mo/GaAs system at temperatures higher than 850°C shows drastic changes in the reacted layer as indicated in the HIRBS spectrum of the sample annealed at 900°C for 20 min (Figure 15). This spectrum indicates that both, Ga and As, are now present in the top layer while the Mo content in the reacted layer becomes more uniform. The uniform nature of the GaAs interface is still maintained. Deconvolution of this spectrum is very difficult because of the extensive signal overlapping. XRD analysis on this sample reveals that diffraction peaks from the Mo_3Ga phase disappear while new sets of diffraction peaks emerge. One set of the peaks can be identified as those from the monoclinic $MoAs_2$ phase (a_o=9.069 Å, b_o=3.2996 Å, c_o=7.717 Å and β=119.37°) while the other set of peaks do not match with those of the existing powder diffraction data from any of the binary Mo-Ga or Mo-As phases.

Suh et al[14] have explored high temperature annealing of the Mo/GaAs system. They found that at annealing temperatures higher than 850°C, a new phase is formed. Using AES and SIMS (secondary ion mass spectrometry) analysis, they concluded that this is a ternary phase with composition Mo_3GaAs_2. Their XRD results on this ternary phase match reasonably well with the new phase identified in the same temperature range in the present study. The structure and the exact composition of this ternary phase are still not well known. But from the HIRBS analysis, it is likely that this ternary phase is the result of the transformation of the Mo_3Ga phase as more As diffuses to the top layer at high temperatures.

HIRBS determination of the quantity of reacted GaAs for Mo/GaAs system undergoing isochronic annealing at temperatures below 700°C reveals that the rate of reaction depends a linearly with the annealing time. Figure 16

shows plots of ln x versus ln t where x is the amount of reacted GaAs in molecules/cm^2 and t is the annealing time in min. Note that for 650°C annealing the slope of the plot is ≈1 indicating that the reaction rate is proportional to time. This linear reaction rate has been observed in the formation of many refractory metal disilicides such as $TiSi_2$, VSi_2, $CrSi_2$, $NbSi_2$, $MoSi_2$, WSi_2, etc. This type of reactions is said to be controlled by the rate of reaction at the M-MSi_2 interface[23-25]. The exact mechanism leading to this linear growth rate is still not understood. However, recent work of refractory metals deposited on Si[26] in high vacuum (<10^{-7} Torr) resulted in parabolic growth rate of the disilicide instead of the linear rate observed in previous studies. This led to the speculation that the presence of native oxide at the metal/silicon interface is responsible for the different growth rate for refractory metal silicides. For M/GaAs reactions, this linear growth rate has not been reported. This may be due to the fact that the native oxide on GaAs is thinner than that on Si and thus normally does not play an important role in M/GaAs reactions.

Figure 16 also shows a plot of ln x versus ln t for annealing at 700°C. The slope for this plot is ≈0.5 which shows that the reaction is diffusion controlled as observed for other metal/GaAs reactions studied in this work. The reactions at temperatures higher than 700°C proceed very rapidly. We believe that these are nucleation controlled reactions as observed in the formation of $NiSi_2$ [Reference 24], $IrSi_2$ [Reference 27], Rh_4Si_5 and Rh_3Si_4 [Reference 28] and the high temperature annealing of the Ir/GaAs contact[29]. This process happens at high temperatures (usually higher than 700°C) when the diffusing atoms are so mobile that diffusion is very rapid. As a result the reactions are no longer controlled by

diffusion but are controlled by the nucleation process which occurs at the interface.

7. W/GaAs

Among the single element metal/GaAs interfaces, the W/GaAs interface is the most inert one. Glancing angle RBS spectra of samples of 180 Å W/GaAs as deposited and annealed at 650, 750, 800 and 900 °C are shown in Figure 17. Below 650 °C no changes can be detected in the RBS spectra. At annealing temperatures between 650 and 800 °C, interdiffusion of W and GaAs is observed. The W diffusion profiles in GaAs at various temperatures were measured by RBS. The activation energy of W diffusion in GaAs is found and equals E=1.87±0.65 eV with the prefactor D_o=7.3X10^{-7}cm^2/s.

Possible reactions between W and GaAs are observed for samples annealed at temperatures >850 °C. Atomic compositions of the reaction products cannot be determined by RBS because of the non-abrupt nature of the backscattering spectra. The RBS spectrum of the thick W layer (1800 Å) on GaAs annealed at 900 °C shows no change for the outer ~1500 Å of W. Reactions between W and GaAs are confined to the ~300 Å of W at the interface.

In addition to the RBS measurements, SEM and TEM were also performed on the W/GaAs system. From these results, it can be concluded that this contact is thermally very stable. Interdiffusion of W and GaAs occurs at the interface at temperatures higher than 600 °C. Upon heat treatment at temperatures higher than 800 °C, macroscopic reactions are initiated at the interface forming islands of W_2As_3 phase resulting in a very rough interface. A schematic diagram for the structure of the contact as it proceeds through ever higher annealing temperatures is shown in Figure 18.

IV. SYSTEMATICS OF SOLID PHASE REACTIONS AT THIN FILM REFRACTORY METAL/GAAS INTERFACES

1. Reaction Kinetics

Diffusion controlled kinetics are observed in all of the refractory M/GaAs (RM/GaAs) reactions at temperatures below 700 °C except for the Mo/GaAs interface. For the case of Mo/GaAs, the reaction rate is found to be linear with time. Such a dependence is usually explained with an interface controlled reaction and has been observed in the formations of refractory metal disilicides. This is consistent with the relatively high temperatures (≥650 °C) needed to induce the solid-state reactions at the Mo/GaAs interface. The high temperature (>700 °C) phase transformations of the Mo/GaAs contact also deviate from the diffusion limited process. At such high temperatures diffusions of both, the metal atoms and the substrate Ga and As atoms are so rapid that the reactions are no longer limited by the diffusion process. Instead, nucleation at the metal/GaAs interface becomes the dominant rate limiting process. When this occurs, the phase growth does not proceed in a layer by layer fashion but as columns at a very rapid rate.

The activation energies for refractory M/GaAs reactions are in the range of 1.25-2.6 eV. These values are comparable to those found for silicide formation indicating similar processes for the M/GaAs and M/Si interface reactions. For the more reactive RM/GaAs systems, for example Ti/GaAs and Zr/GaAs, the activation energies are typically less than 1.7 eV. For the less reactive V/GaAs and Nb/GaAs systems (and possibly the Mo/GaAs), the activation energies are higher than 2 eV.

2. Interface Reactivity

Reactivity of the thin film RM/GaAs interfaces is related to the nature of the metal layers. Near noble metals which have high electronegativity and weak metal-metal bonds (and thus have low heat of vaporization) are found to be more reactive than the electropositive refractory metals which have strong M-M bonds[30]. Primarily two major driving forces can be identified for the solid phase reactions at the M/GaAs interface: 1) the M-M bond strength which is manifested in the heat of vaporization (or heat of formation) of the metals; and 2) the electronegativity differences between the metal and the Ga and As. Electronegativity difference of a molecule A-B in the Pauling's scale is defined as the square root of the difference between the actual bond energies D(A-B) and the arithmetic (or geometric) mean of the corresponding symmetrical bond energies[31]. Thus, it is reasonable to assume that the interface reactivity of an interface is directly dependent on the sum of the square of the electronegativity differences of M-Ga and M-As and inversely dependent on the heat of vaporization ΔH of the metal. Consequently, one can define a reactivity parameter R in the following way:

$$R \sim \frac{(X_M - X_{Ga})^2 + (X_M - X_{As})^2}{\Delta H} . \qquad (2)$$

Hence, an interface with a high R value is very reactive and vice versa.

Figure 19 shows a plot of the activation energy for interface reactions for the R.M/GaAs systems studied in the present work versus the logarithm of R. Data on the near noble metal/GaAs interfaces are also

shown as open circles[30] in the figure. The refractory metal/GaAs systems follow a linear relationship. The near noble metal/GaAs contacts do not display a simple relationship between R and ΔE. Thus it can be concluded that for reactions at RM/GaAs interfaces, the reactivities follow equation (2). The activation energies for these systems depend on their corresponding R values in the following way:

$$E = C + K\ln(R) \qquad (3)$$

where the values of C and K can be deduced from the plot in figure 19. A least square fit for data in figure 19 yields $C \approx -2.3$ and $K \approx 1.3$. Alternatively one can express the reactivity as $R \sim \exp(-\Delta E/1.3)$.

3. Phase Distribution

Distribution of the different phases formed in M/GaAs reactions is found to follow an electronegativity rule: for $|X_M - X_{Ga}| \neq |X_M - X_{As}|$, phase stratification with a layer sequence of M-Ga/M-As/GaAs occurs always. For the cases of the refractory metals Ti, Zr, V, Nb, Cr and W, we find $|X_M - X_{Ga}| < |X_M - X_{As}|$. The metal is the relatively electropositive species in comparison to the As. Therefore the metal diffuses to the interface and preferentially reacts with As forming M-As at the interface. The Ga released in the M-As reaction reacts with the indiffusing metal atoms forming a layer of M-Ga on top of the M-As phase.

The Mo/GaAs contact is an exception to the above rule . Molybdenum has X=1.8 and hence should react similarly to Co[32,33] and Ni[34-36] forming M_xGaAs ternary phase. However, Mo/GaAs reactions which are induced at

high temperatures result in the formation of stratified Mo-Ga and Mo-As phases. This may be due to the high reaction temperatures at which the the GaAs at the interface is dissociated and thermally induced interdiffusion occurs. It is possible that the diffusion coefficient of Ga in Mo is much higher than that of As in Mo at this temperature which would account for the observed phase stratification. Unfortunately, diffusion coefficient data for Ga and As in Mo are not available for comparison.

In addition to the electronegativity rule mentioned above, phase stratification in M/GaAs systems is also dependent on the thickness of the reacted layer. When the grain size of the reacted phases is comparable or larger than the reacted layer thickness, the phases can only be laterally separated in order to minimize interface energy. As has been discussed above, the grain size of the reacted phases is, in turn dependent on the M-M bond strength of the metal.

V. SUMMARY AND CONCLUSIONS ON REFRACTORY METAL/GAAS REACTIONS

1. Phase composition and structure

1) Except for Mo, the final stable phases are always binary (M_xGa and M_yAs where $x \geq 1$ and $y \leq 1$). For Ti, Zr and V the stable M_xGa phases have hexagonal structure with x ranging from 1 to 1.7. The stable phases for the Mo/GaAs system are believed to be the binary $MoAs_2$ and the ternary Mo_xGaAs_y with $x \approx 3$ and $y \approx 2$. The exact composition and structure of this ternary phase is still unknown.

2) The ratio of the amount of reacted metal to GaAs, [M]/[GaAs] in the final reacted layer is normally ≥ 1.5. This does not apply to

the W/GaAs system since it is thermally very stable and the reactions occur at the interface at high temperatures are nonuniform. For Ti, Zr, V and Cr, this ratio is 2.

3) For systems which react in two stages, the intermediate phases formed are binary phases. These intermediate phases are most commonly the cubic M_3Ga phases as observed for the V, Cr and Mo cases.

2. Phase distribution and morphology

1) Vertical phase distribution is always observed for all RM/GaAs systems except for W/GaAs. This can be explained by the M-M bond strength argument. Since refractory metals have stronger M-M bonds than the near noble metals, and therefore larger heats of vaporization, grain size in the reacted layer is smaller. Thus phase stratification is energetically more favorable.

2) Phase distribution in the reacted layer is also determined by the electronegativity of the deposited metal. The large electronegativity difference between electropositive refractory metals ($X<1.8$) and As results in relatively immobile As at the GaAs interface and thus stratification of phases in the sequence of M-Ga/M-As/GaAs.

3) The interfaces between different phases are normally nonuniform. This is not surprising since the refractory metals normally have electronegativity in between those of Ga and As so that in many cases they are attracted to both the Ga and As atoms resulting in severe interpenetration of the M-Ga and M-As phases.

3. Reaction kinetics

1) Initial reactions at refractory metal/GaAs interfaces do not begin at temperatures lower than 450°C. This high reaction temperature is also a result of the electropositive nature of these metals. Therefore, the RM/GaAs interfaces are said to be relatively inert.

2) Diffusion controlled reaction rates dominate thin film RM/GaAs solid phase reactions with activation energies in the range of 1.25 to 2.6 eV. An exception is the initial reaction of Mo/GaAs which is interface reaction rate controlled and the high temperature phase transformation of Mo/GaAs which are nucleation controlled.

3) Interface reactivity of RM/GaAs systems depends primarily on the M-M bond strength of the metal and the electronegativity differences between metal and the substrate Ga and As. An empirical relationship between the activation energies for RM/GaAs reactions and an interface reactivity parameter R defined by equation 3 has been established (equation 3).

ACKNOWLEDGMENTS

The authors gratefully acknowledge the technical assistance of W. L. Searles for the maintainance of the RBS facility at LBL. The sputter depositions of the metal films and the plasma enhanced chemical deposition of the SiO_2 caps were performed by S. K. Cheung. The HIRBS measurements were made possible through the assistance and cooperation of R. Stokstad, R. M. Larimer and the staff of the 88" cyclotron at LBL. One of the authors (KMY) would like to thank Dr. T Sands of Bell Communications Research, Inc. for many inspiring discussions on metal/GaAs systems.

This work was supported by the Director, Office of Basic Energy Sciences, Materials Science Division of the U. S. Department of Energy under Contract No. DE-AC03-76SF00098.

REFERENCES

1. N. Yokoyama, T. Minura, M. Fukuta and H. Ishikawa, 1981 International Solid State Circuits Conference Digest of Technical Papers, p.218 (1981).
2. K. Matsumoto, N, Hashizume, H. Tanoue and T. Kanayama, Jpn. J. Appl. Phys. **21**, L393 (1982).
3. N. Yokoyama, T. Ohnishi, K. Odani and M. Abe, IEEE International Electron Devices Meeting Technical Digest, p. 80 (1981).
4. W. F. Tseng and A. Christou, IEEE International Electron Device Meeting Technical Digest, p. 174 (1982).
5. J. K. Truman and P. H. Holloway, J. Vac. Sci. Technol. **A3**, 992 (1985).
6. N. Yokoyama, T. Ohnishi, T. Nukamura and H. Nishi, Mat. Res. Soc. Symp. Proc. **54**, 401 (1986).
7. T. Ohnishi, N. Yokoyama, H. Onodera, S. Suzuki and A. Shibatomi, Appl. Phys. Lett. **43**, 600 (1983).
8. Z. Zhu, N. W. Cheung, Z. V. Lemnois, M. D. Strathman and S. B. Stimmell, J. Vac. Sci. Technol. **B4**, 1398 (1986).
9. A. Callegari, G. D. Spiers, J. H. Magerlein, H. C. Guthrie, J. Appl. Phys. **61**, 2054 (1987).
10. J. R. Waldrop, Appl. Phys. Lett. **43**, 87 (1983)
11. H. Yamagishi, Jpn. J. Appl. Phys. **23**, L895 (1984).
12. N. Uchitomi, M. Nagaoka, K. Shimada, T. Mizoguchi and N. Toyada, J. Vac. Sci. Technol. **B4**, 1392 (1986).

13. A. E. Geissberger, R. A. Sadler, F. A. Leyenaar and M. L. Balzan, J. Vac. Sci. Technol. **A4**, 3091 (1986).

14. O. Wada, S. Yanagisawa and H. Takanashi, Appl. Phys. Lett. **29**, 263 (1976).

15. S. D. Mukherjee, D. V. Morgan, M. J. Howes, J. G. Smith and P. Brook, J. Vac. Sci. Technol. **16**, 138 (1979).

16. S. D. Mukherjee, C. J. Palmstrom and J. G. Smith, J. Vac. Sci. Technol. **17**, 904 (1980).

17. P. Ling, J-K. Chang, M-S. Lin and J-C. Lou, Mat. Res. Soc. Symp Proc. **48**, 137 (1985).

18. K. Suh, H. K. Park and K. L. Moazed, J. Vac. Sci. Technol. **B1**, 365 (1983).

19. K. M. Yu, S. K. Cheung, T. Sands, J. M. Jaklevic, N. W. Cheung and E. E. Haller, J. Appl. Phys. **60**, 3235 (1986).

20. K. M. Yu, J. M. Jaklevic and E. E. Haller, Nucl. Instrum. Meth. **B10/11**, 606 (1985).

21. K. M. Yu, M. S. Thesis, University of California, Berkeley (1984), LBL #18897.

22. T. Sands, V. G. Keramidas, K. M. Yu, J. Washburn and K. Krishnan, to be published, J. Mat. Res. (1987).

23. K. N. Tu and J. W. Mayer, "Silicide Formation" in *Thin Film-Interdiffusion and Reactions*, eds. J. M. Poate, K. N. Tu and J. W. Mayer, Chapter 10 (Wiley, New York, 1978).

24. F. M. d'Heurle and P. Gas, J. Mat. Res. **1**, 205 (1986).

25. L. D. Locker and C. D. Capio, J. Appl. Phys. **44**, 4366 (1973).

26. L. S. Hung, J. Gyulai and J. W. Mayer, J. Appl. Phys. **54**, 5076 (1983).

27. C. S. Petersson, J. E. Baglin, W. Hammer, F. M. d'Heurle, T. S. Kuan, I. Odhmari, J. deSousa Pires and P. A. Tove, J. Appl. Phys. **50**, 3357 (1979).

28. C. S. Petersson, R. Anderson , J. E. Baglin, J. Dempsey, W. Hammer, F. M. d'Heurle and S. J. Laplaca, J. Appl. Phys. **51**, 373 (1980).

29. K. M. Yu, T. Sands, J. M. Jaklevic and E. E. Haller, to be published, J. Appl. Phys. (1987).

30. K. M. Yu, Ph. D. Thesis, University of California, Berkeley (1987).

31. L. Pauling, *The Nature of Chemical Bonds*, Cornell University Press, Ithaca, 1960.

32. A. J. Yu, G. J. Galvin, C. J. Palmstrom and J. W. Mayer, Appl. Phys. Lett. **47**, 934 (1985).

33. A. J. Yu, G. J. Galvin, J. W. Mayer, C. J. Palmstrom, T. Sands and C. C. Chang, presented at the 1986 Spring meeting of the Mat. Res. Soc., April 17, 1986, Palo Alto, Ca.

34. M. Ogawa, J. Appl. Phys. **51**, 406 (1980).

35. T. Sands, V. G. Keramidas, J. Washburn and R. Gronsky, Appl. Phys. Lett. **48**, 402 (1986).

36. A. Lahav, M. Eisenberg and Y. Komen, Mat. Res. Soc. Symp. Proc. 37, 641 (1985).

Table I **Summary** of the solid phase reactions between thin film refractory metals and (100) GaAs substrate.

Metal	Reaction Temp. (°C)	Phases formed	Phase Distribution	Reaction Rate[a)]	Activation Energy (eV)
Ti	>400	TiGa (Tetragonal) TiAs (Hexagonal)	TiGa/TiAs/GaAs	D	1.53 ±0.15
Zr	450	Zr_xGa } $x+y \approx 3$ Zr_yAs	$Zr_xGa/Zr_yAs/GaAs$	D	1.25 ±0.10
	700	Zr_5Ga_3 (Hexagonal) Zr_xAs; $x \approx 0.4$	$Zr_5Ga_3/Zr_xAs/GaAs$		
V	450	V_3Ga (Cubic) V_xAs; $x \approx 2$	$V_3Ga/V_xAs/GaAs$	D	2.10 ±0.10
	700	V_6Ga_5 (Hexagonal) V_4As_3 (Monoclinic)	$V_6Ga_5/V_4As_3/GaAs$		
Nb	550	Nb_xGa } $x<y$; Nb_yAs $x+y \approx 1.5$	$Nb_xGa/Nb_yAs/GaAs$ (non-abrupt interface)	D	2.60 ±0.30
Cr	≥450	Cr_3Ga (Cubic) CrAs (Orthorhombic)	$Cr_3Ga/CrAs/GaAs$	-	-
	550	CrGa (Rhombohedral) CrAs (Orthorhombic)	CrGa/CrAs/GaAs	-	-
Mo	≥650	Mo_3Ga (Cubic) Mo_5As_4 (Tetragonal)	$Mo_3Ga/Mo_5Ga_4/GaAs$	D,R	-
	≥850	Mo_xGaAs_y $MoAs_2$ (Monoclinic)	(?)	N	-
W	≥750	W_2As_3 (Monoclinic)	"ball up" forming islands of single grain W_2As_3.	-	-

a) D≡diffusion controlled growth; R≡interface reaction comntrolled growth and N≡nucleation controlled growth.

Table II Comparison of the XRD data[a)] for Ti/GaAs samples under different annealing conditions and the powder diffraction data of TiGa and TiAs from the JCPDS diffraction file.

XRD data		Powder diffraction data		
450 °C, 20 min.	500 °C, 20 min.	Ti[b)]	TiGa[c)]	TiAs[b)]
2.78 (w)	2.786 (m)		2.807(110)	2.79 (102)
	2.46 (w)			2.479(103)
2.28 (s)	2.2815(s)		2.292(111)	
	2.174 (w)			2.183(104)
	1.8154(m)			1.823(110)
	1.69 (w)			1.693(106)
	1.33 (w)		1.323(221)	1.320(205)
1.243(w)		1.247(112)		
	1.14 (w)		1.14 (222)	

a) All plane spacings are in Å. Powder diffraction data are indexed with hkl in paratheses. (w), (m) and (s) denote weak, medium and strong intensity diffraction peaks, respectively.

b) Powder diffraction data for Ti and TiAs are taken from JCPDS card # 5-0682 and 7-134, respectively.

c) Powder diffraction data for TiGa are calculated from the crystallographic parameters obtained from the equilibrium phase diagram of Ti-Ga.

Table III Comparison of XRD data[a)] for annealed Zr/GaAs samples with powder diffraction data for Zr_5Ga_3 from the JCPDS file.

Zr/GaAs XRD data		Powder diffraction data
650 °C, 30 min.	700 °C, 60 min.	Zr_5Ga_3[b)]
	3.1596 (m)	3.456 (200)
	2.975 (m)	
2.923 (w)		
	2.8237 (w)	
2.75 (m)		
2.68 (w)		
2.609 (s)	2.60 (m)	2.603 (210,102)
	2.30 (w)	2.299 (300,112)
	1.996 (m)	1.998 (220)
1.899 (w)	1.8997 (m)	1.918 (310,212) 1.881 (221)
1.561 (w)	1.54 (w)	1.536 (213,321)
1.30 (m)		
	1.2276 (w)	

a) All plane spacings are in Å. Powder diffraction data are indexed with hkl in paratheses. (w), (m) and (s) denote weak, medium and strong intensity diffraction peaks, respectively.

b) Powder diffraction data for Zr_5Ga_3 is taken from card # 12-82 of the JCPDS powder diffraction data file.

Table IV A summary of the HIRBS data from annealed V/GaAs samples showing 2-stage reactions.

	Reacted mater.	Atomic conc. in reacted phases	
	[V]/[GaAs]	[V]/[Ga]	[V]/[As]
stage 1	5.0 ±0.1	3.0 ±0.1	2.0 ±0.1
stage 2	2.2 ±0.2	1.2 ±0.1	1.1 ±0.1

FIGURE CAPTIONS

Figure 1 (a) HIRBS spectra of 1000 Å Ti/GaAs sample as deposited and annealed at 450 and 500°C for 20 min. (b) Deconvolution of the spectrum of the sample annealed at 500°C for 20 min showing a layer sequence of Ti-Ga/Ti-As /GaAs.

Figure 2 HIRBS spectra of 1100 Å Zr/GaAs samples as deposited and annealed at different temperatures.

Figure 3 Plots of the square of GaAs consumed during Zr/GaAs reactions as measured by HIRBS versus annealing time for different annealing temperatures. The linear relationship shown in these plots indicate that the reactions are diffusion controlled.

Figure 4 An Arrhenius plot of the diffusivities as deduced from the slopes of the plots in Figure 4.3 versus the annealing temperatures in degree Kelvin. The activation energy of Zr/GaAs reactions is obtained from the slope of this plot and is =1.25±0.10 eV.

Figure 5 HIRBS spectra of 1500 Å V/GaAs samples as deposited and annealed at 600°C for 20 min and 700°C for 30 min.

Figure 6 Deconvolution of the HIRBS spectra of the two annealed samples (600°C, 20 min and 700°C, 30 min) indicating layer sequence of V-Ga/V-As/GaAs for both samples with different V-Ga and V-As phases detected.

Figure 7 Plots of the square of GaAs consumed during V/GaAs reactions as measured by HIRBS versus annealing time for different temperatures.

Figure 8 An Arrhenius plot of the diffusivities versus the annealing temperatures for V/GaAs reactions. Activation energy obtained from this plot is =2.1±0.1 eV.

Figure 9 A series of HIRBS spectra of 550 Å Nb/GaAs samples as deposited and annealed at 600 and 700°C for 20 min.

Figure 10 A schematic diagram of the final structure of Nb/GaAs reactions as estimated from the HIRBS results.

Figure 11 A series of HIRBS spectra of 1200 Å Cr/GaAs samples as deposited, annealed at 450°C for 20 min, 550°C for 10 min and 600°C for 20 min.

Figure 12 Deconvolution of the HIRBS spectra of Cr/GaAs samples annealed at 550°C for 10 min (a) and 600°C for 20 min (b) reveals the two layer structures in the samples. The two annealed samples represent two stages of complete reactions of the Cr/GaAs system.

Figure 13 A series of HIRBS spectra of 1500 Å Mo thin film on GaAs samples as deposited, annealed at 700°C for 40 min, 700°C for 140 min and 850°C for 200 min.

Figure 14 Deconvolution of the HIRBS spectrum of the Mo/GaAs sample annealed at 700°C for 140 min. Well defined layer sequence of Mo-Ga/Mo-As/GaAs is clearly observed.

Figure 15 HIRBS spectrum of Mo/GaAs sample annealed at 900°C for 20 min showing drastic changes in the features as compared to the spectrum of samples annealed at lower temperatures.

Figure 16 Plots of the reacted GaAs thickness as a function of the annealing time in the logarithm scale for Mo/GaAs reactions at 650 and 700°C. The slopes of the plots indicate that the reactions at 650°C (slope =1) are reaction rate limited and the reactions at 700°C (slope=0.5) are diffusion limited.

Figure 17 (a)-(e) Glancing angle RBS spectra of 180 Å W/GaAs samples as deposited and annealed for 20 min at 650, 750, 800, and 900°C.

Figure 18 Schematic diagrams for the structural evolution of the W/GaAs contact as it proceeded through ever higher annealing temperatures.

Figure 19 A plot of the activation energies for interface reactions for M/GaAs systems studied in the present work versus the logarithm of the reactivity parameters R as calculated from equation (6.1). The open circles are data from near noble metals and the full circles are from refractory metals.

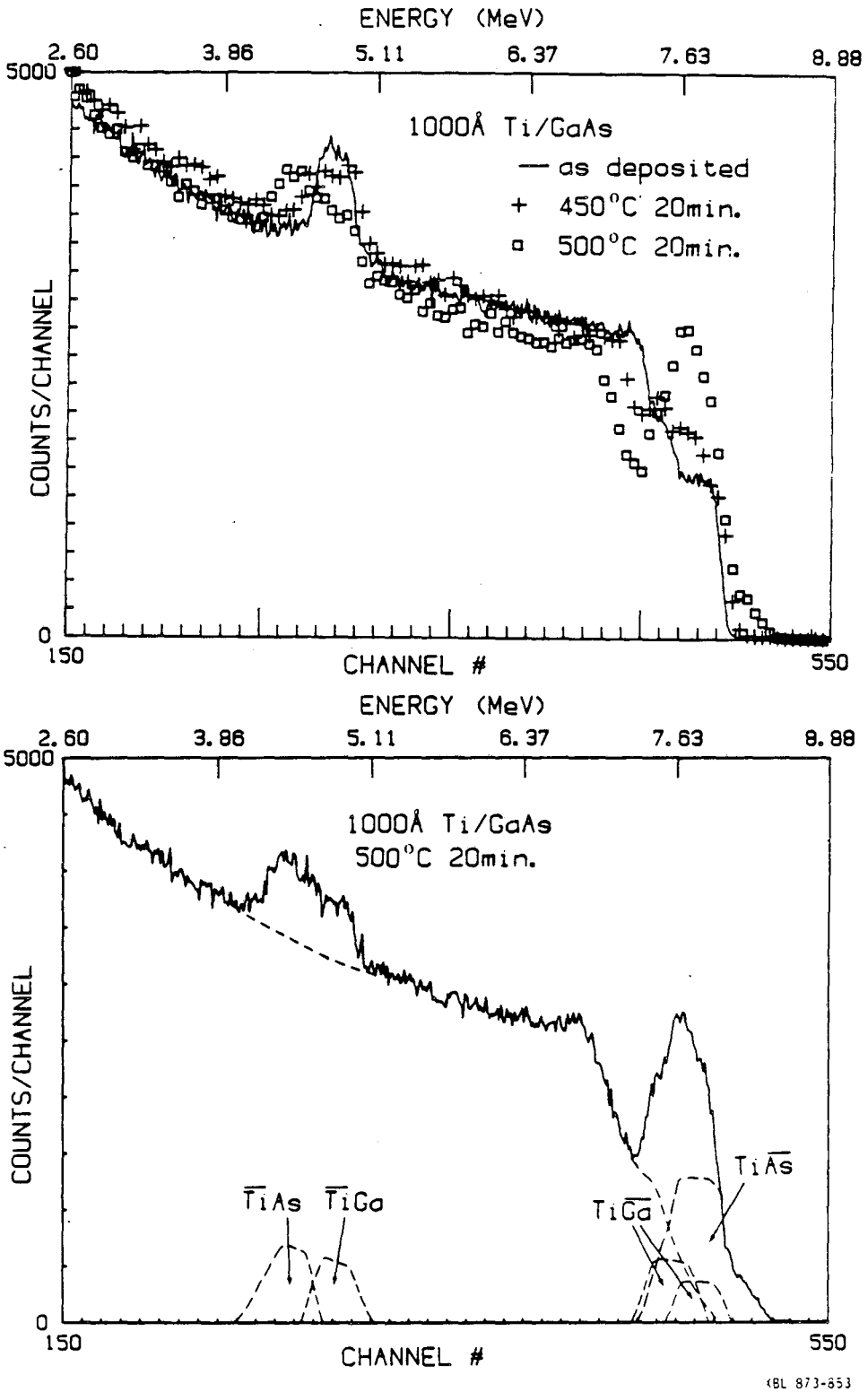
ENERGY (MeV)
2.60
3.86
5.11
6.37
7.63
8.88
5000
0
COUNTS/CHANNEL
1000Å Ti/GaAs
— as deposited
+ 450°C 20min.
□ 500°C 20min.
150
CHANNEL #
550
ENERGY (MeV)
2.60
3.86
5.11
6.37
7.63
8.88
5000
0
COUNTS/CHANNEL
1000Å Ti/GaAs
500°C 20min.
TiAs
TiGa
TiGa
TiAs
150
CHANNEL #
550
CBL 873-853

Fig. 1

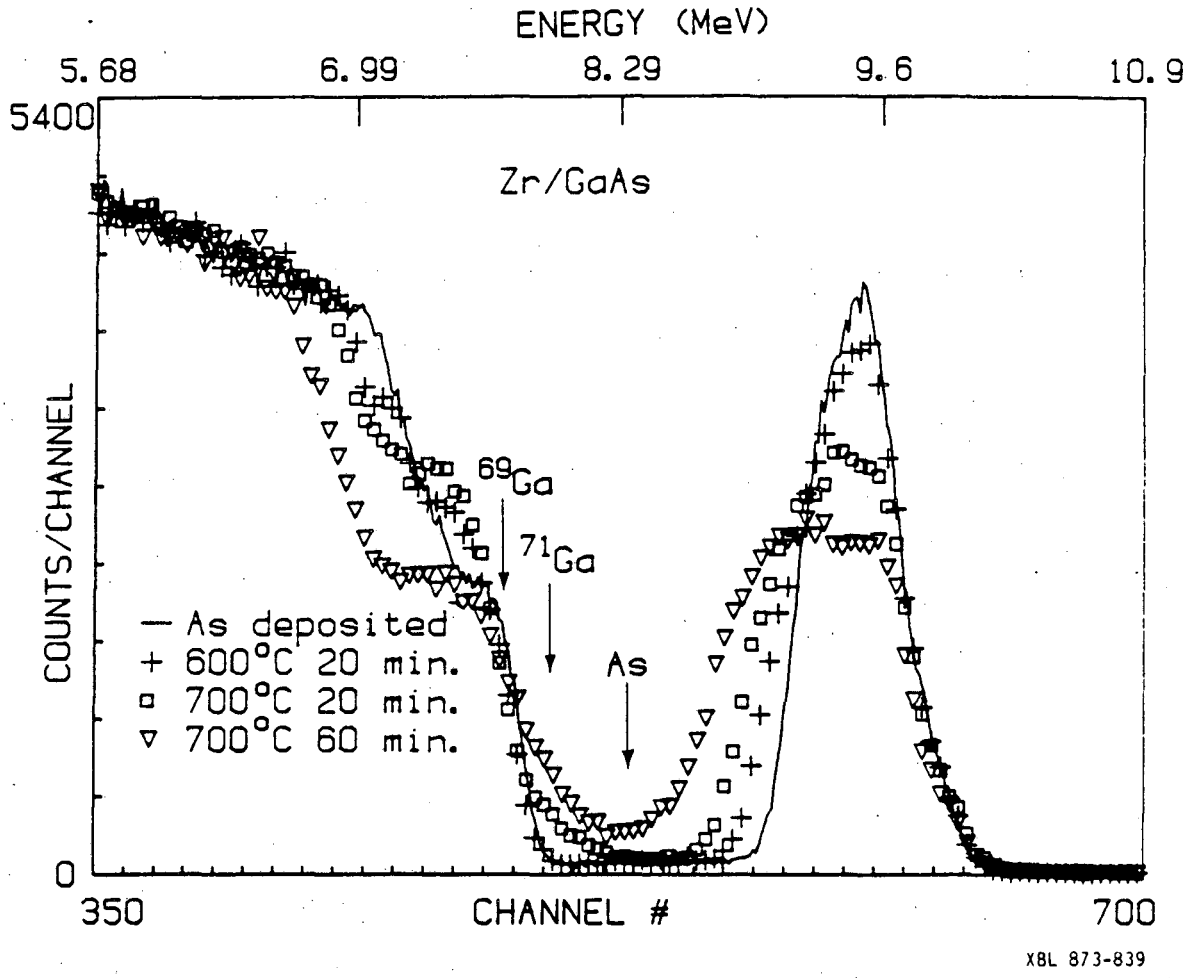
ENERGY (MeV)
5.68
6.99
8.29
9.6
10.9
5400
0
Zr/GaAs
COUNTS/CHANNEL
69Ga
71Ga
As
— As deposited
+ 600°C 20 min.
▫ 700°C 20 min.
▽ 700°C 60 min.
350
CHANNEL #
700
XBL 873-839

Fig. 2

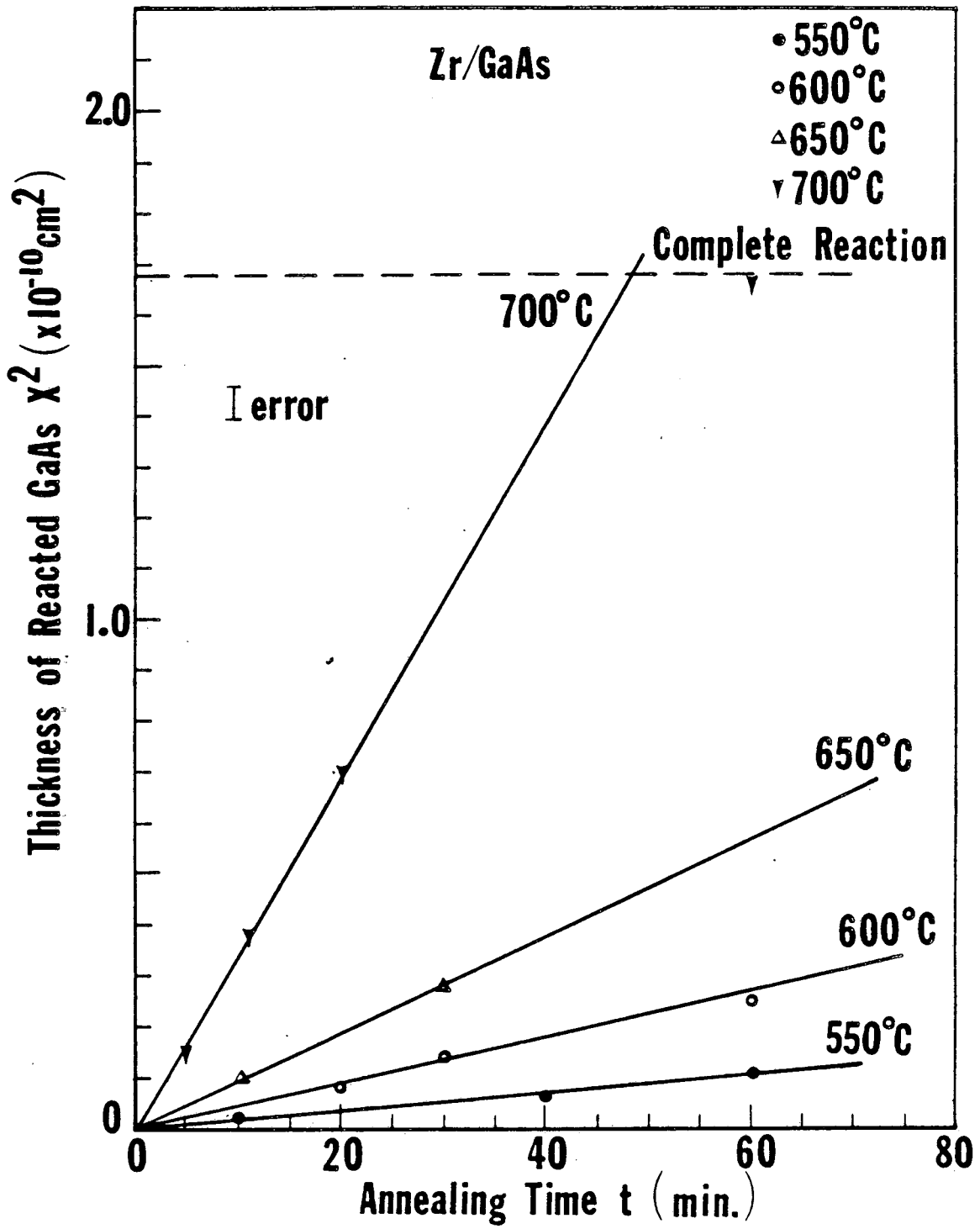

XBL 872-564

Fig. 3

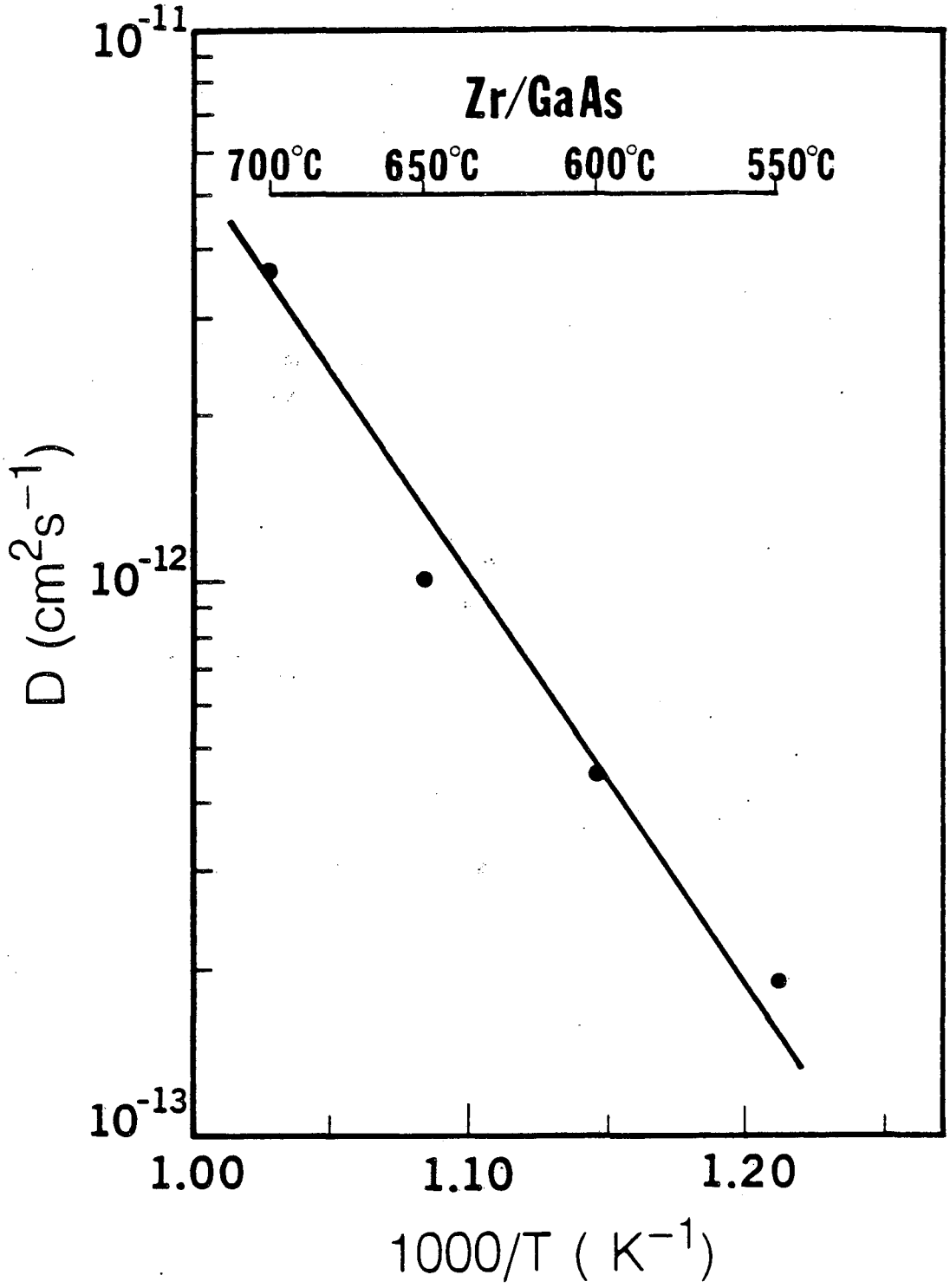

XBL 873-848

Fig. 4

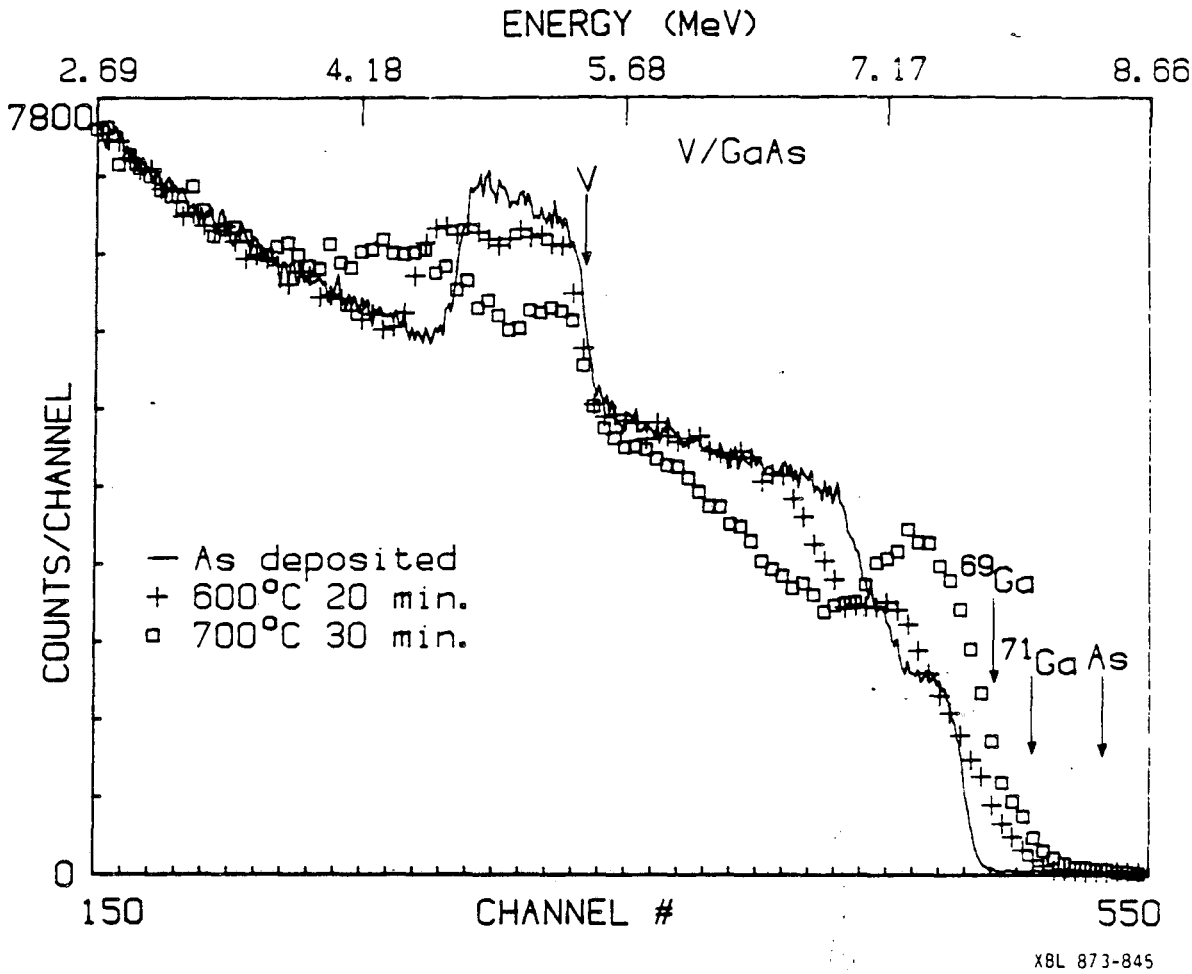
ENERGY (MeV)
2.69
4.18
5.68
7.17
8.66
7800
0
V/GaAs
V
COUNTS/CHANNEL
— As deposited
+ 600°C 20 min.
▫ 700°C 30 min.
69Ga
71Ga
As
150
CHANNEL #
550
X8L 873-845

Fig. 5

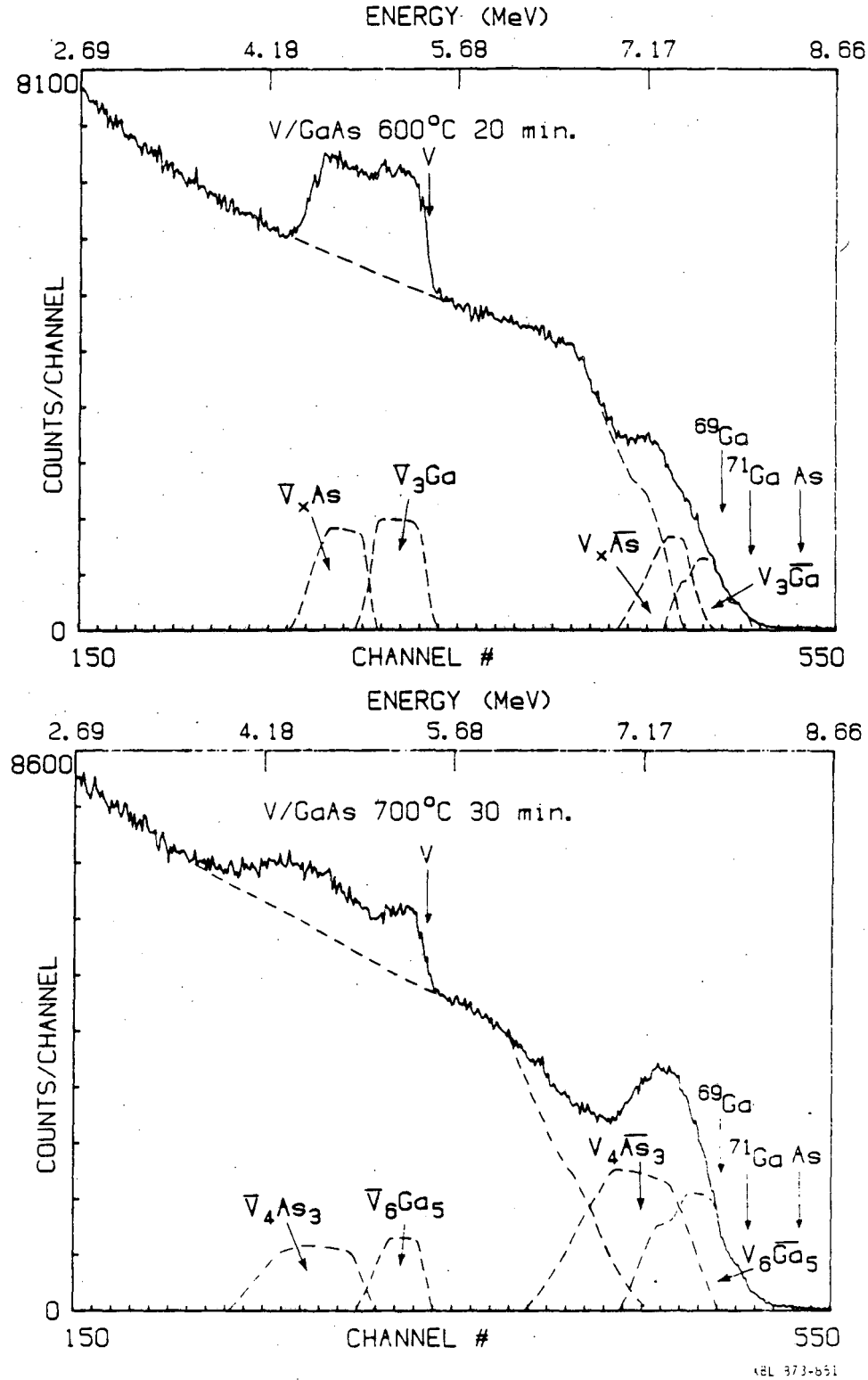
ENERGY (MeV)
2.69
4.18
5.68
7.17
8.66
8100
V/GaAs 600°C 20 min.
V
COUNTS/CHANNEL
69Ga
71Ga
As
V3Ga
VxAs
VxAs
V3Ga
0
150
CHANNEL #
550
ENERGY (MeV)
2.69
4.18
5.68
7.17
8.66
8600
V/GaAs 700°C 30 min.
V
COUNTS/CHANNEL
69Ga
V4As3
71Ga
As
V4As3
V6Ga5
V6Ga5
0
150
CHANNEL #
550

Fig. 6

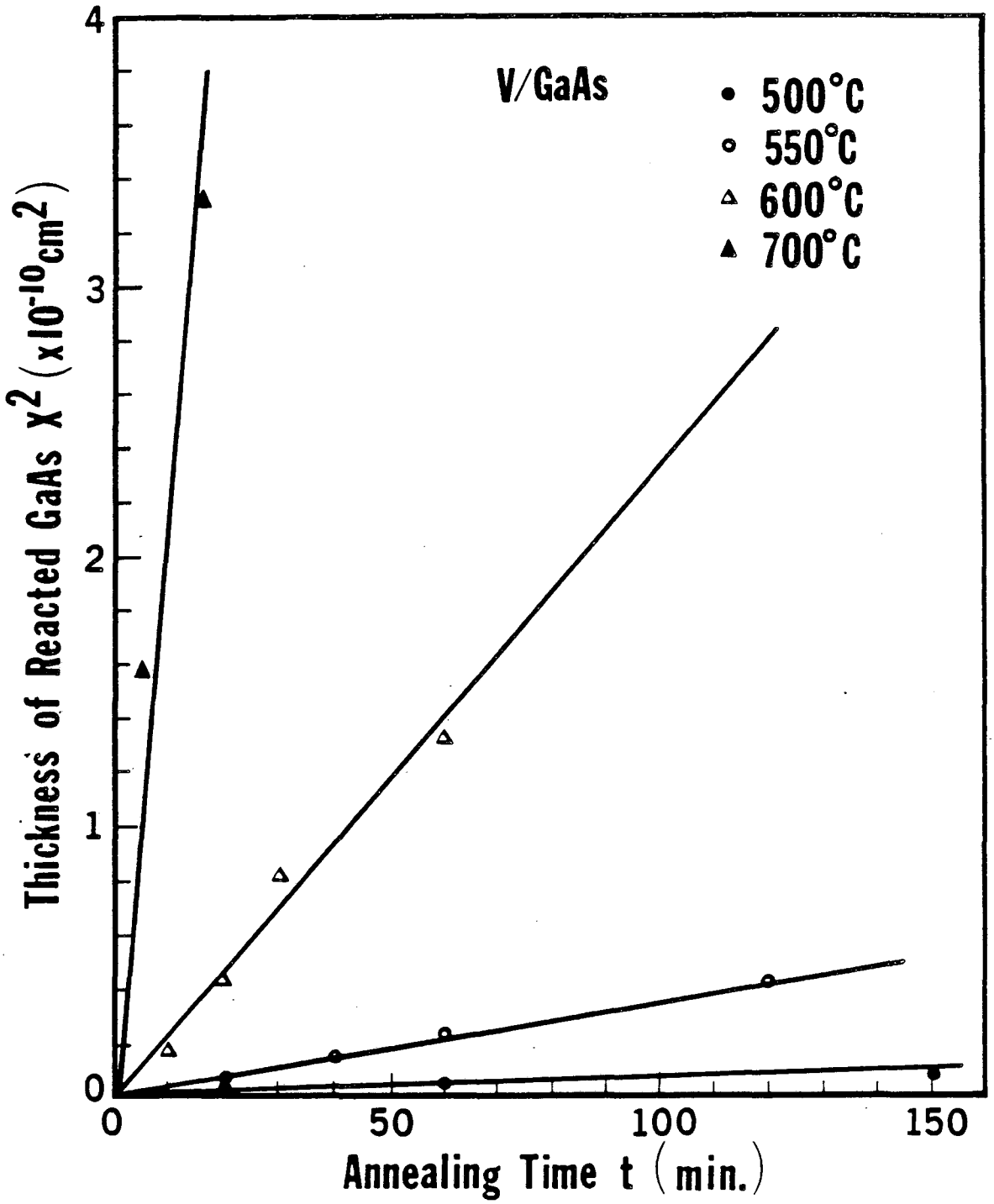

XBL 873-849

Fig. 7

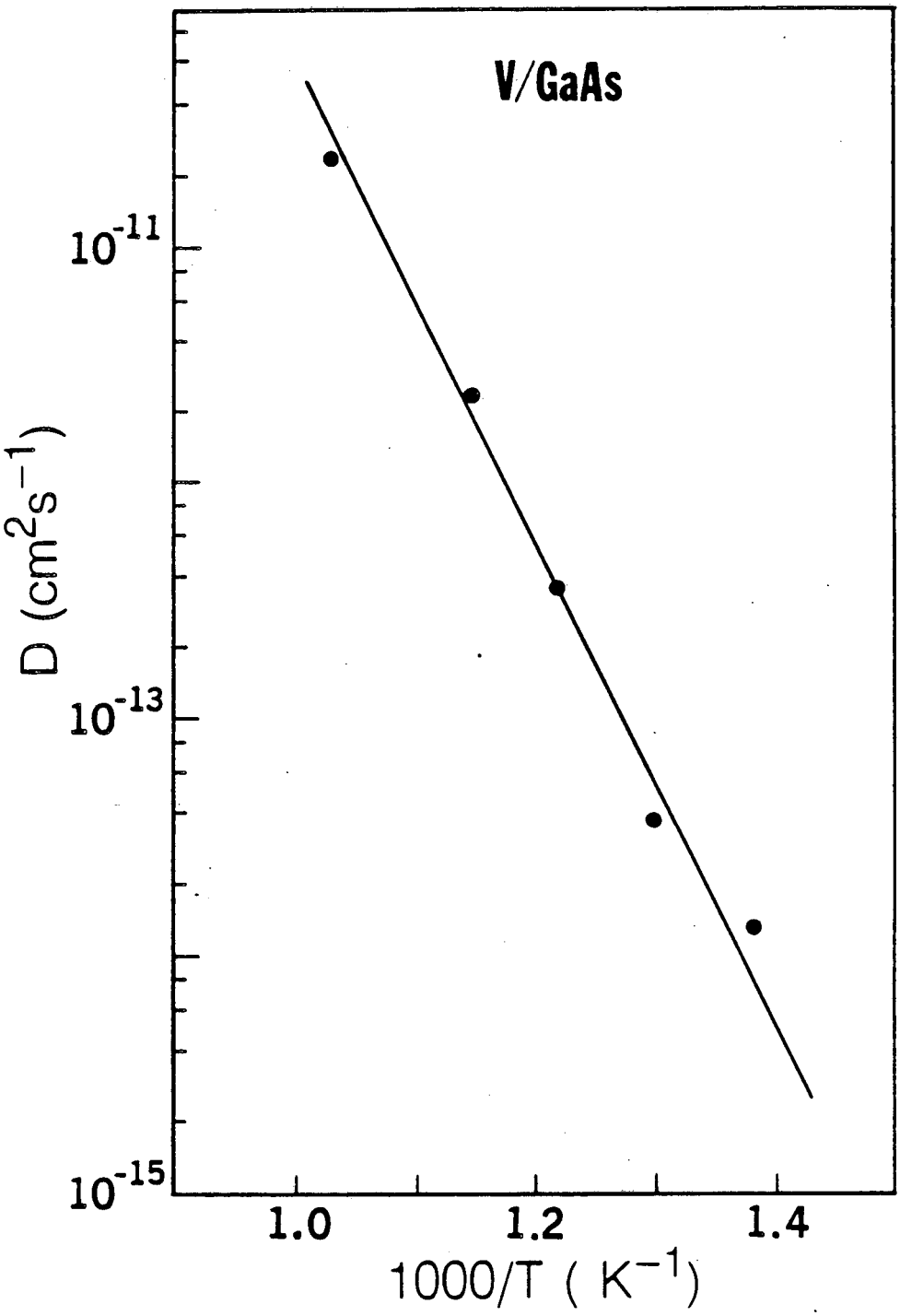

XBL 873-1102

Fig. 8

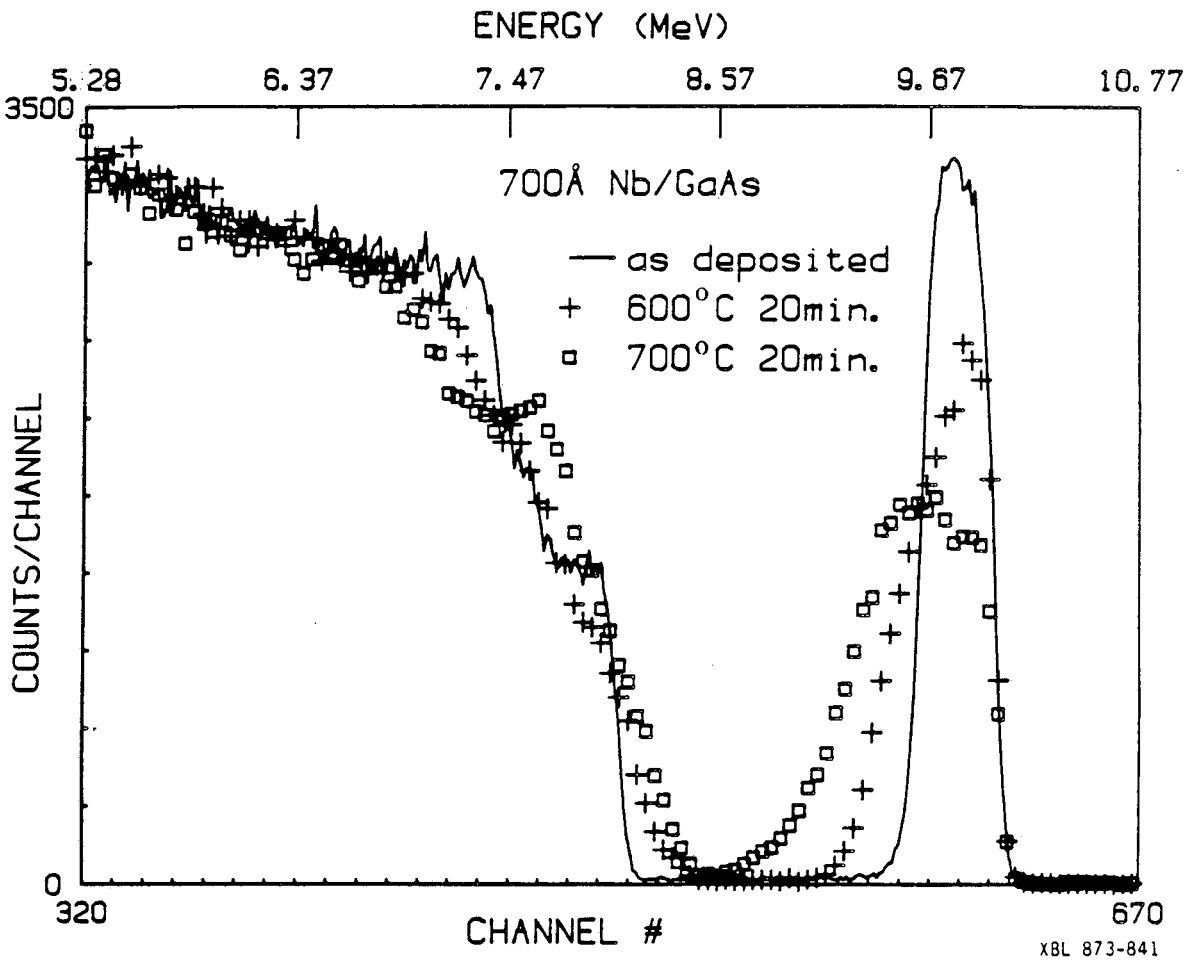
ENERGY (MeV)
5.28
6.37
7.47
8.57
9.67
10.77
3500
0
700Å Nb/GaAs
as deposited
600°C 20min.
700°C 20min.
COUNTS/CHANNEL
320
CHANNEL #
670
XBL 873-841

Fig. 9

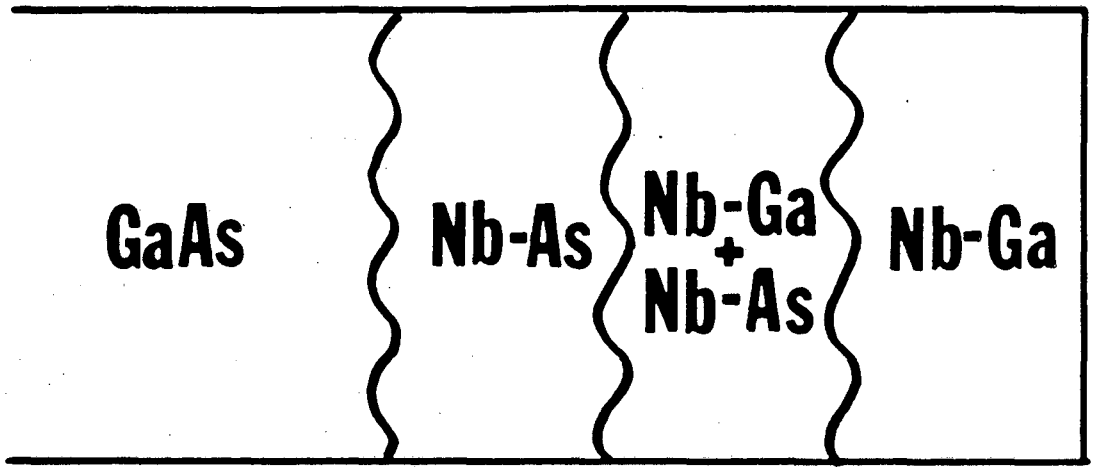

XBL 873-1105

Fig. 10

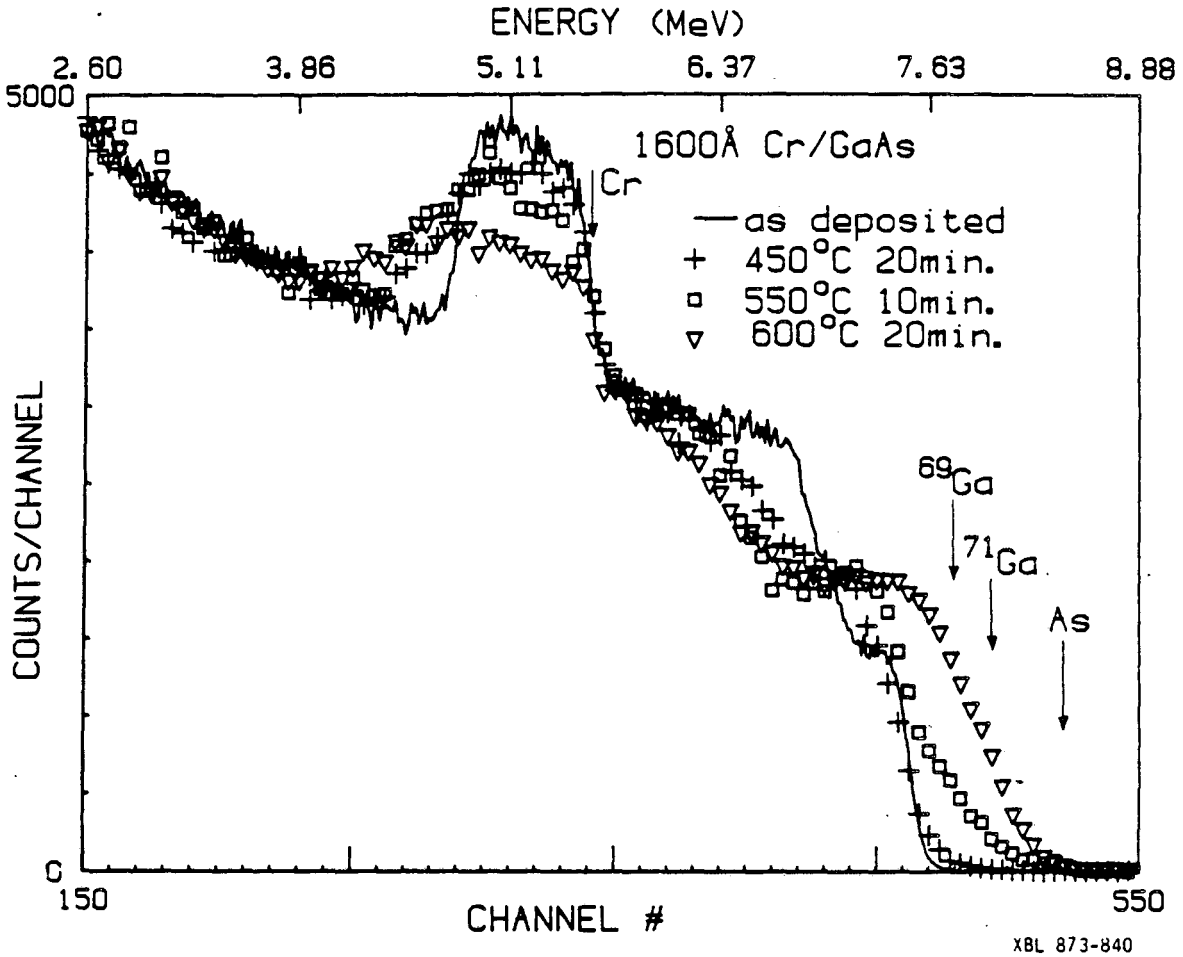
ENERGY (MeV)
2.60
3.86
5.11
6.37
7.63
8.88
5000
0
COUNTS/CHANNEL
1600Å Cr/GaAs
Cr
—as deposited
+ 450°C 20min.
▫ 550°C 10min.
▽ 600°C 20min.
69Ga
71Ga
As
150
550
CHANNEL #
XBL 873-840

Fig. 11

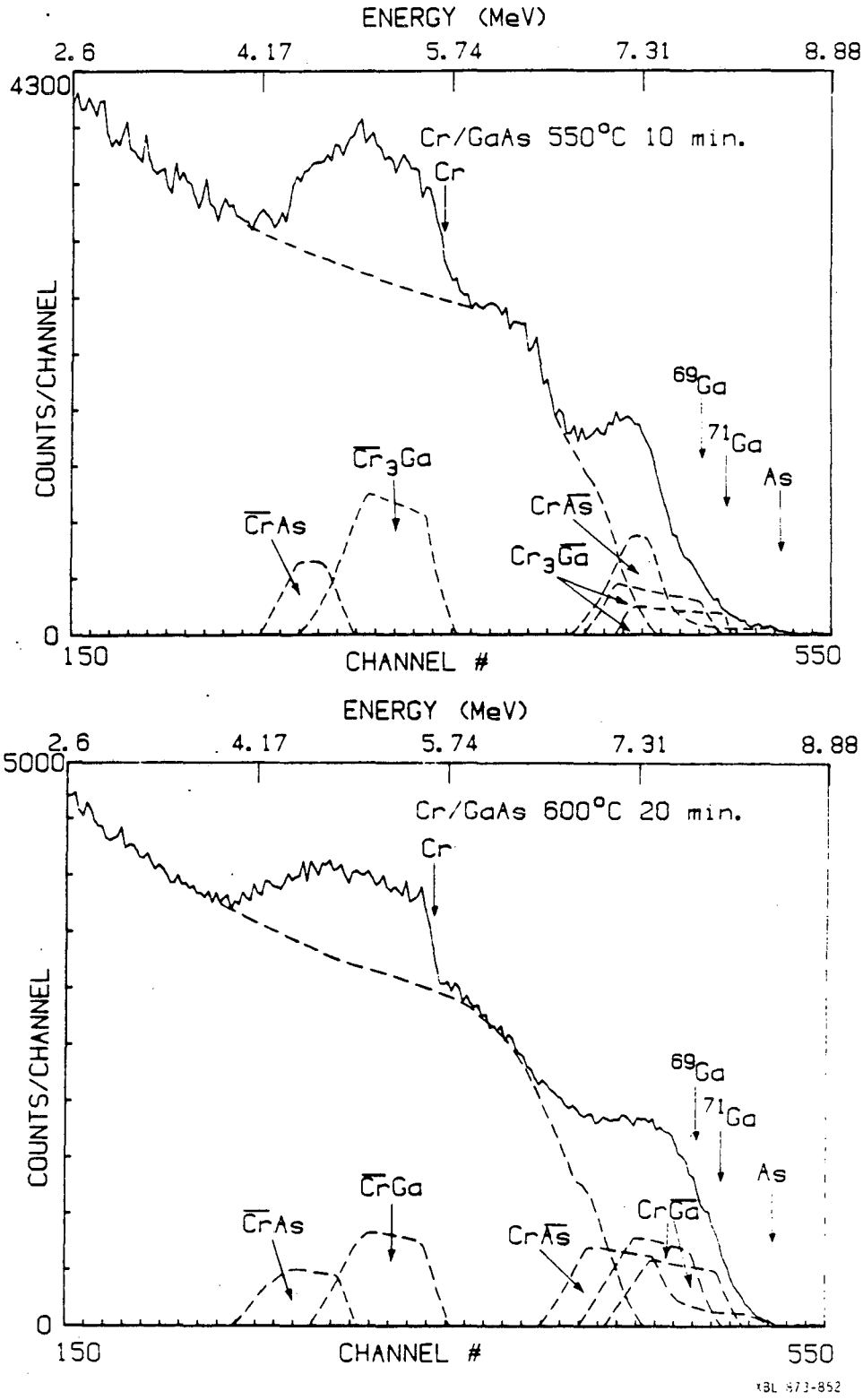
ENERGY (MeV)
2.6
4.17
5.74
7.31
8.88
4300
Cr/GaAs 550°C 10 min.
Cr
COUNTS/CHANNEL
69Ga
71Ga
As
Cr3Ga
CrAs
CrAs
Cr3Ga
0
150
CHANNEL #
550
ENERGY (MeV)
2.6
4.17
5.74
7.31
8.88
5000
Cr/GaAs 600°C 20 min.
Cr
COUNTS/CHANNEL
69Ga
71Ga
As
CrGa
CrAs
CrAs
CrGa
0
150
CHANNEL #
550
XBL 873-852

Fig. 12

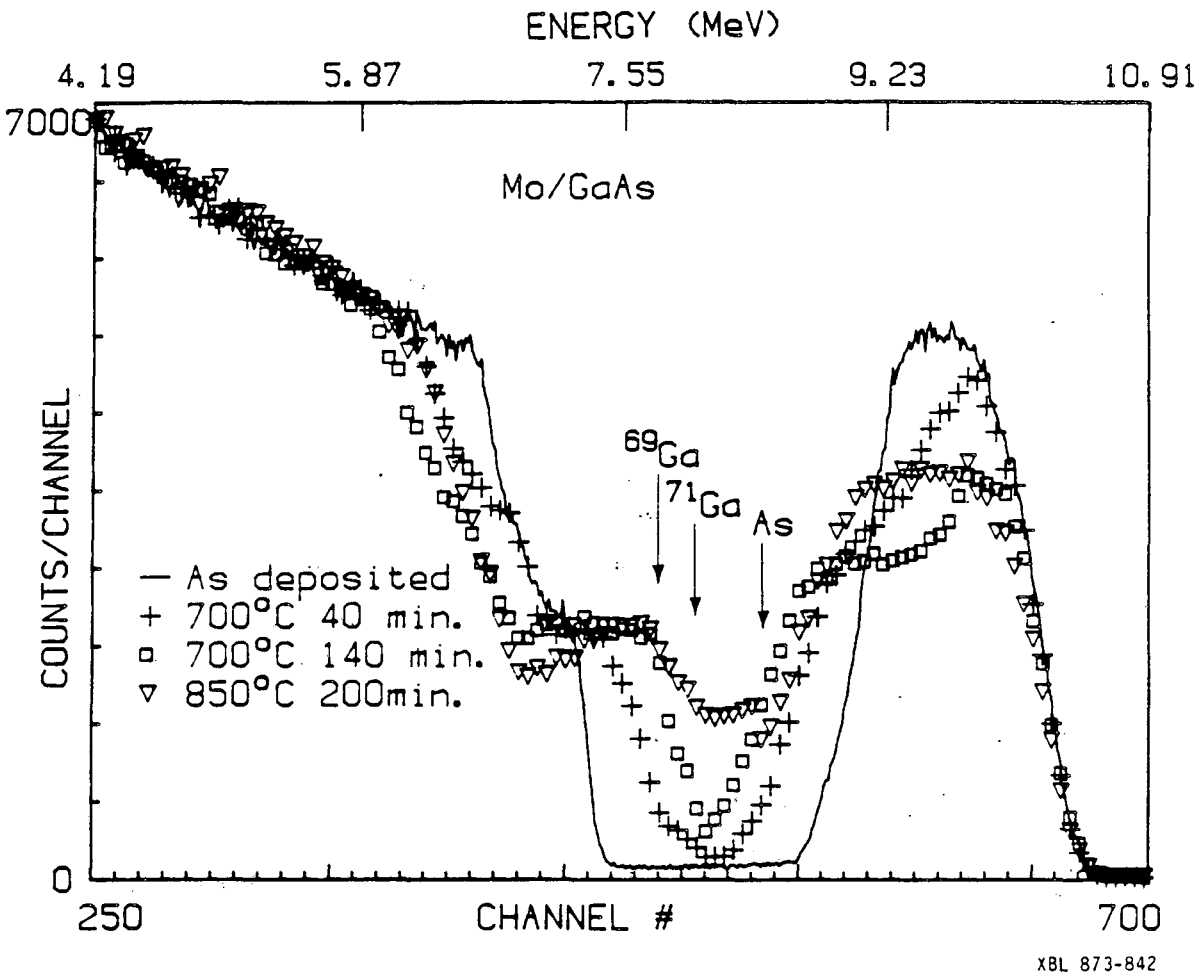
ENERGY (MeV)
4.19
5.87
7.55
9.23
10.91
7000
0
Mo/GaAs
COUNTS/CHANNEL
69Ga
71Ga
As
— As deposited
+ 700°C 40 min.
▫ 700°C 140 min.
▽ 850°C 200min.
250
CHANNEL #
700
XBL 873-842

Fig. 13

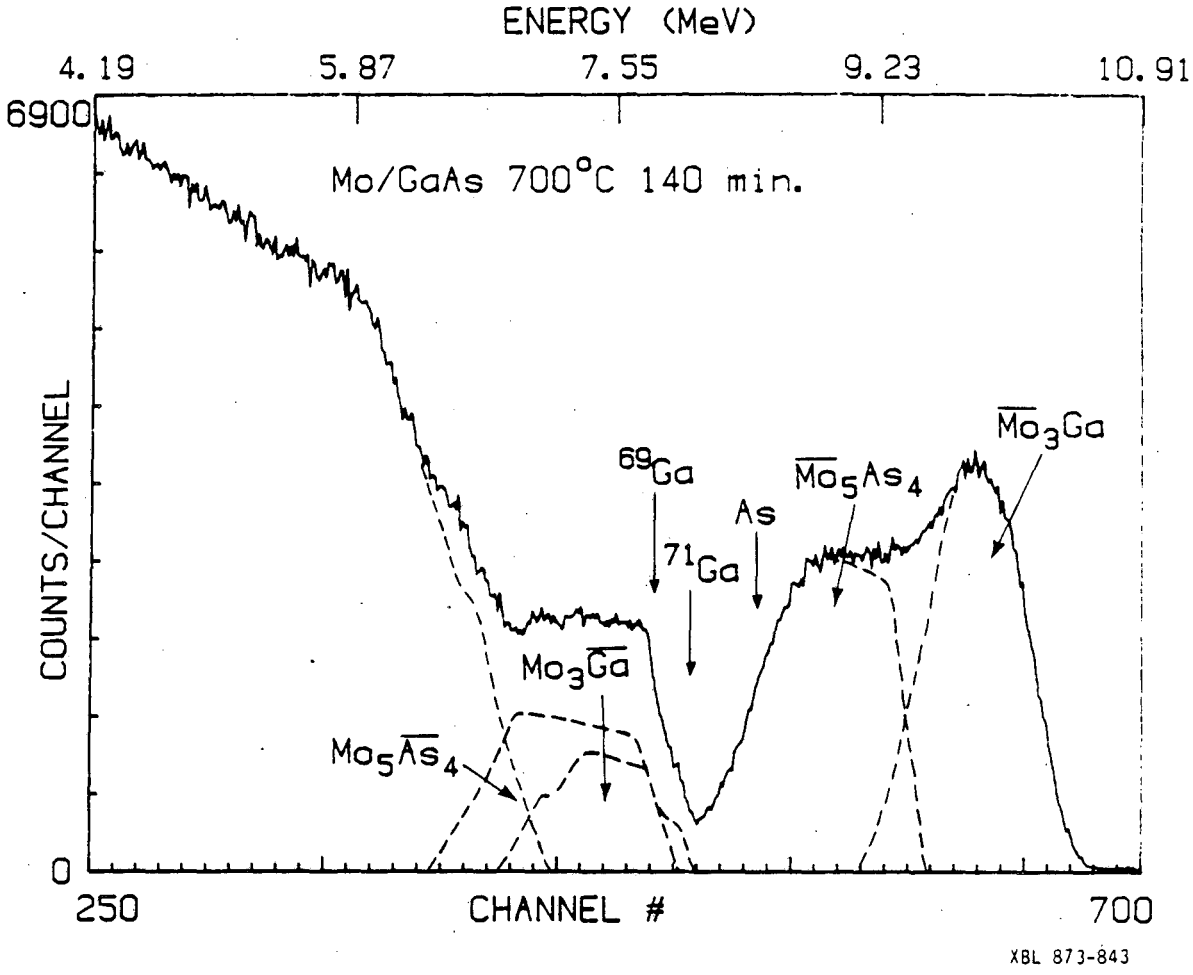
ENERGY (MeV)
4.19
5.87
7.55
9.23
10.91
6900
0
COUNTS/CHANNEL
Mo/GaAs 700°C 140 min.
69Ga
71Ga
As
Mo5As4
Mo3Ga
Mo3Ga
Mo5As4
250
CHANNEL #
700
XBL 873-843

Fig. 14

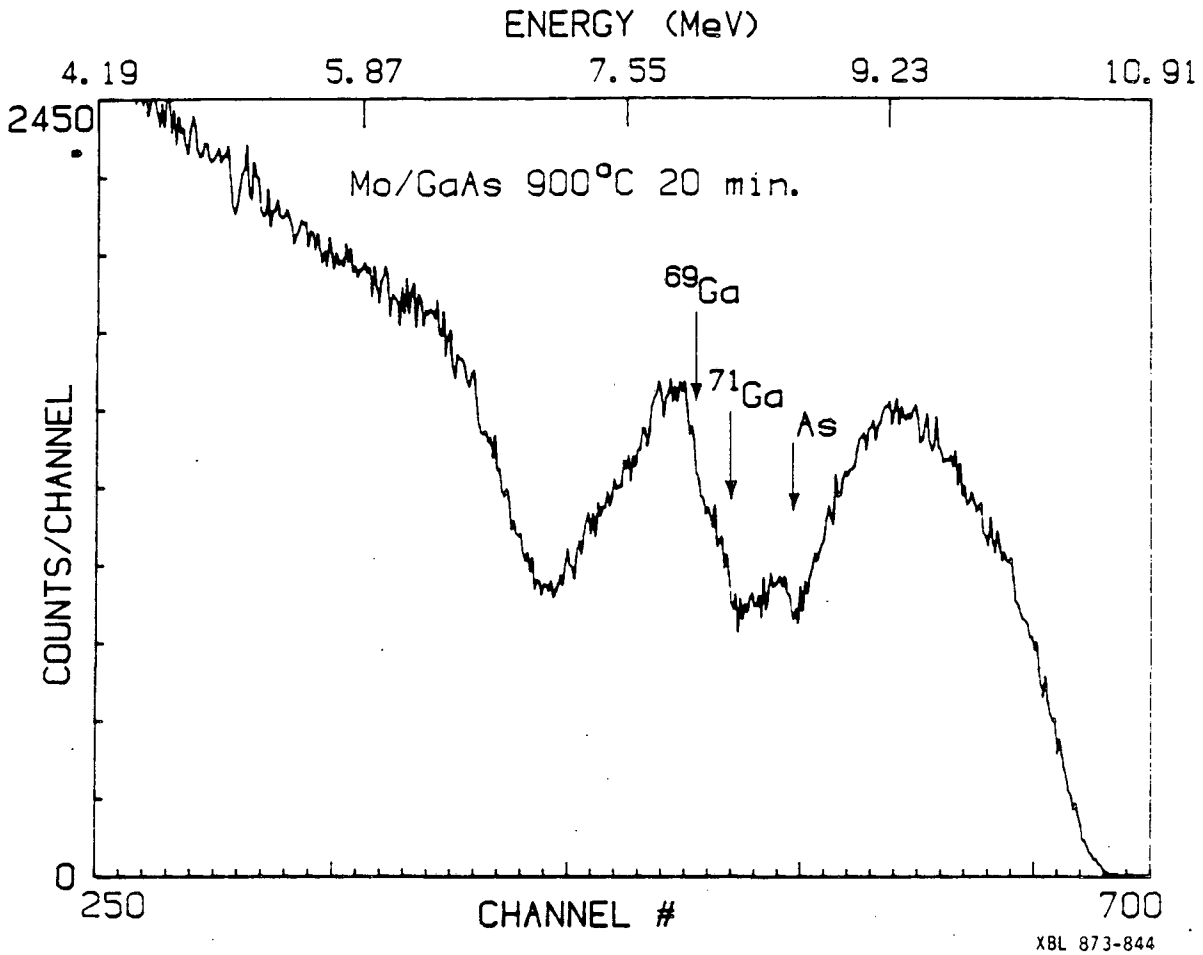
ENERGY (MeV)
4.19
5.87
7.55
9.23
10.91
2450
0
COUNTS/CHANNEL
Mo/GaAs 900°C 20 min.
69Ga
71Ga
As
250
CHANNEL #
700
XBL 873-844

Fig. 15

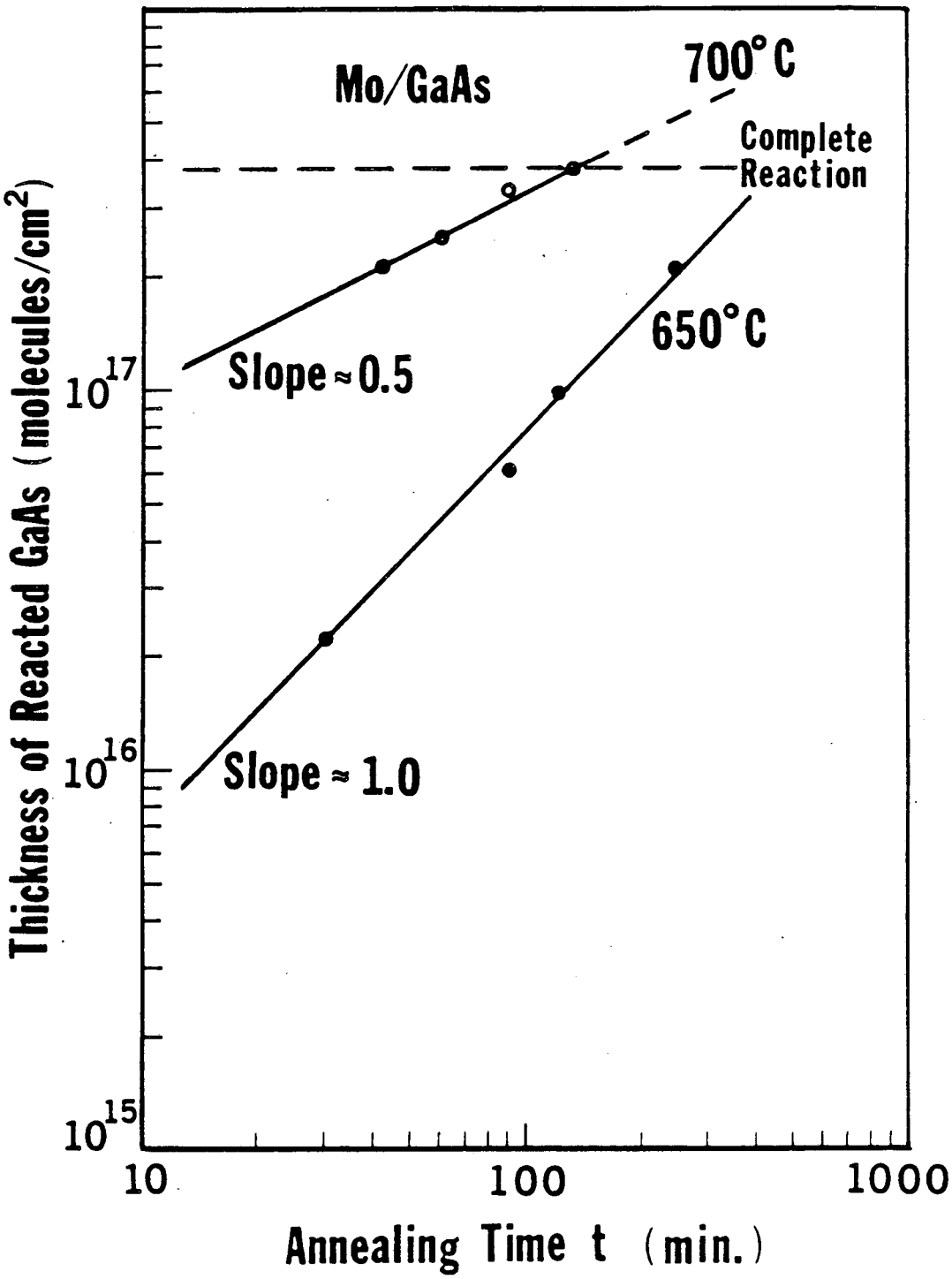

XBL 872-563

Fig. 16

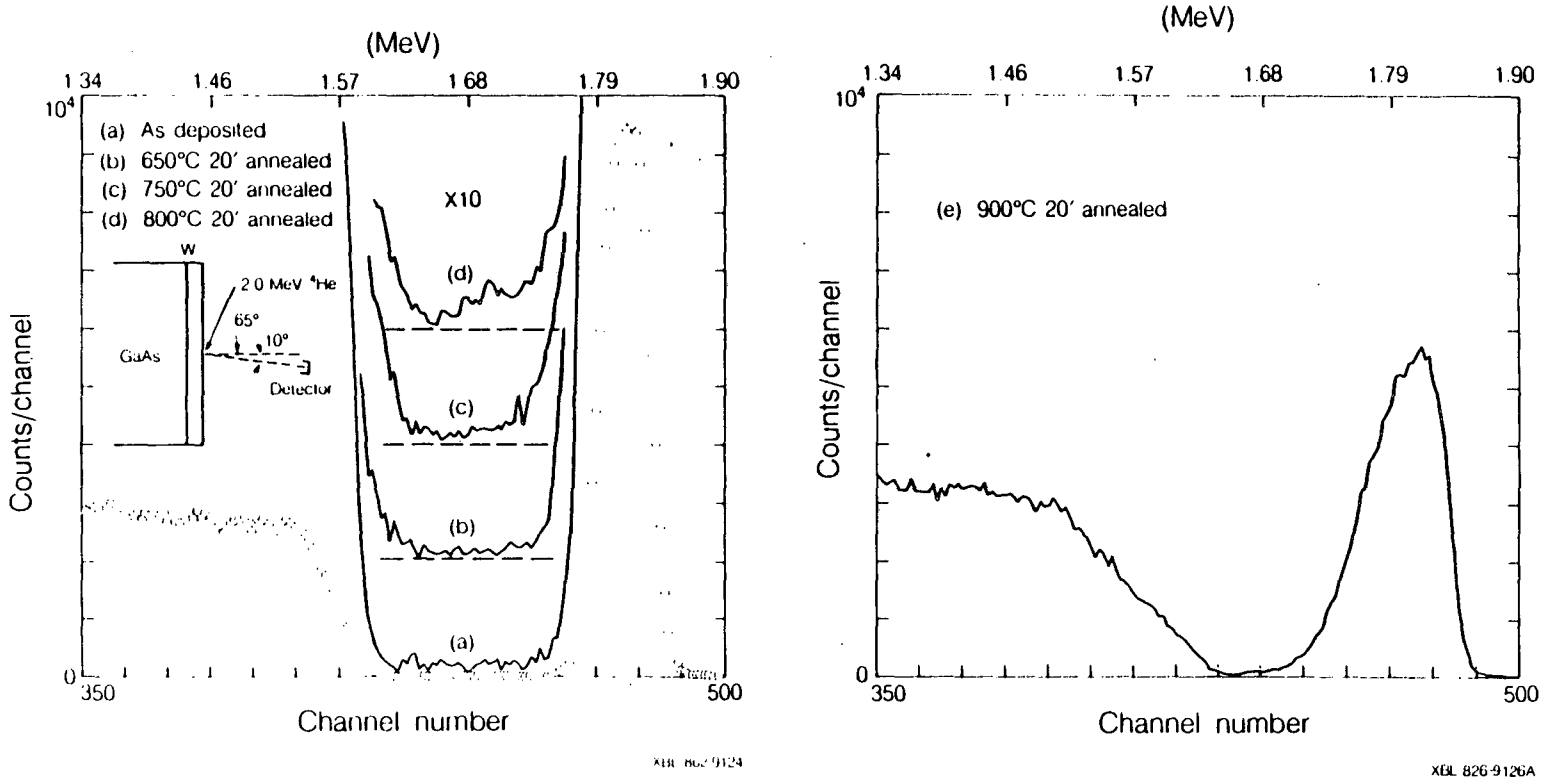
(MeV)
1.34
1.46
1.57
1.68
1.79
1.90
10^4
0
(a) As deposited
(b) 650°C 20′ annealed
(c) 750°C 20′ annealed
(d) 800°C 20′ annealed
W
2.0 MeV ^{4}He
65°
10°
GaAs
Detector
X10
(d)
(c)
(b)
(a)
Counts/channel
350
500
Channel number
XBL 826-9124
(MeV)
1.34
1.46
1.57
1.68
1.79
1.90
10^4
0
(e) 900°C 20′ annealed
Counts/channel
350
500
Channel number
XBL 826-9126A

Fig. 17

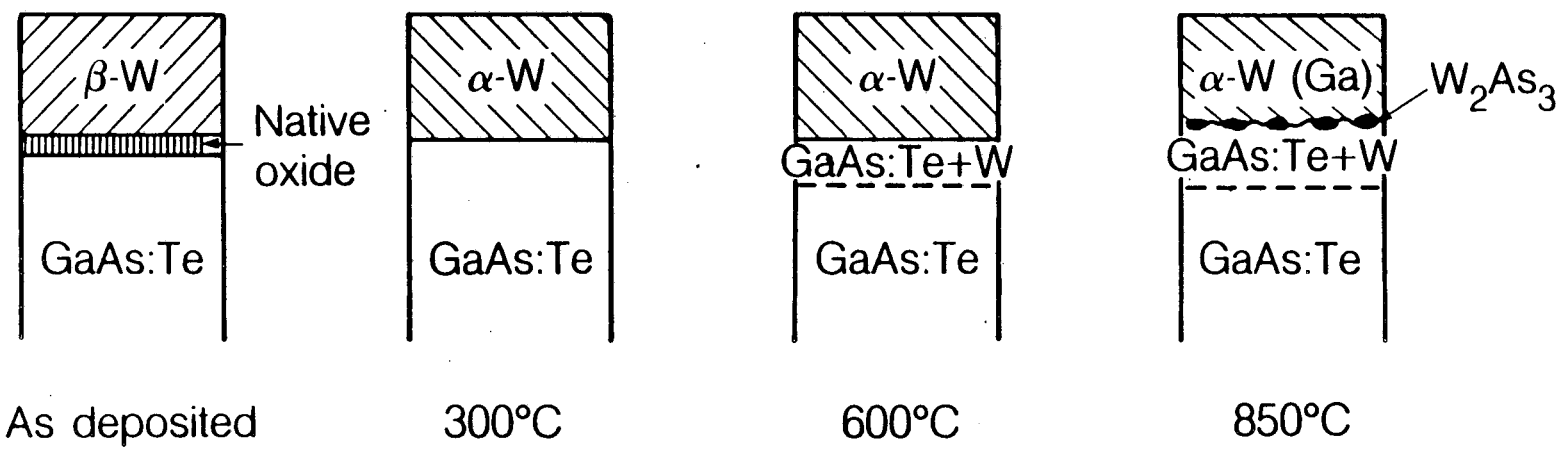

XBL 862-9135

Fig. 18

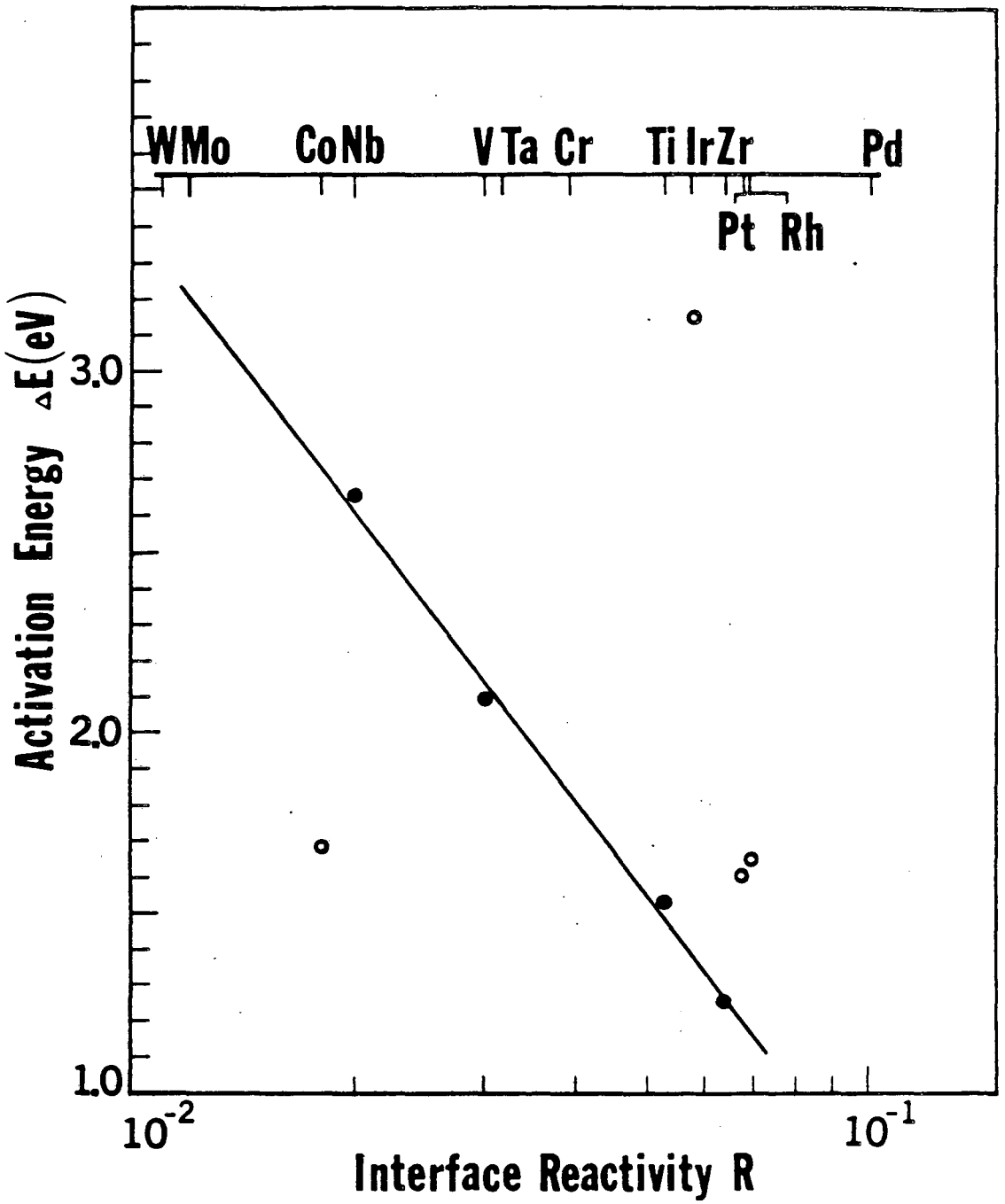

XBL 872-565

Fig. 19

This report was done with support from the Department of Energy. Any conclusions or opinions expressed in this report represent solely those of the author(s) and not necessarily those of The Regents of the University of California, the Lawrence Berkeley Laboratory or the Department of Energy.

Reference to a company or product name does not imply approval or recommendation of the product by the University of California or the U.S. Department of Energy to the exclusion of others that may be suitable.

LAWRENCE BERKELEY LABORATORY
TECHNICAL INFORMATION DEPARTMENT
UNIVERSITY OF CALIFORNIA
BERKELEY, CALIFORNIA 94720